

The Origin of Large Molecules in Primordial Autocatalytic Reaction Networks

Varun Giri¹, Sanjay Jain^{1,2,3*}

1 Department of Physics and Astrophysics, University of Delhi, Delhi, India, **2** Jawaharlal Nehru Centre for Advanced Scientific Research, Bangalore, India, **3** Santa Fe Institute, Santa Fe, New Mexico, United States of America

Abstract

Large molecules such as proteins and nucleic acids are crucial for life, yet their primordial origin remains a major puzzle. The production of large molecules, as we know it today, requires good catalysts, and the only good catalysts we know that can accomplish this task consist of large molecules. Thus the origin of large molecules is a chicken and egg problem in chemistry. Here we present a mechanism, based on autocatalytic sets (ACSs), that is a possible solution to this problem. We discuss a mathematical model describing the population dynamics of molecules in a stylized but prebiotically plausible chemistry. Large molecules can be produced in this chemistry by the coalescing of smaller ones, with the smallest molecules, the 'food set', being buffered. Some of the reactions can be catalyzed by molecules within the chemistry with varying catalytic strengths. Normally the concentrations of large molecules in such a scenario are very small, diminishing exponentially with their size. ACSs, if present in the catalytic network, can focus the resources of the system into a sparse set of molecules. ACSs can produce a bistability in the population dynamics and, in particular, steady states wherein the ACS molecules dominate the population. However to reach these steady states from initial conditions that contain only the food set typically requires very large catalytic strengths, growing exponentially with the size of the catalyst molecule. We present a solution to this problem by studying 'nested ACSs', a structure in which a small ACS is connected to a larger one and reinforces it. We show that when the network contains a cascade of nested ACSs with the catalytic strengths of molecules increasing gradually with their size (e.g., as a power law), a sparse subset of molecules including some very large molecules can come to dominate the system.

Citation: Giri V, Jain S (2012) The Origin of Large Molecules in Primordial Autocatalytic Reaction Networks. PLoS ONE 7(1): e29546. doi:10.1371/journal.pone.0029546

Editor: Petter Holme, Umeå University, Sweden

Received: October 3, 2011; **Accepted:** November 30, 2011; **Published:** January 4, 2012

Copyright: © 2012 Giri, Jain. This is an open-access article distributed under the terms of the Creative Commons Attribution License, which permits unrestricted use, distribution, and reproduction in any medium, provided the original author and source are credited.

Funding: VG received a Senior Research Fellowship from the University Grants Commission, Government of India and from the Department of Biotechnology, Government of India. SJ received support from the Department of Biotechnology, Government of India. The funders had no role in study design, data collection and analysis, decision to publish, or preparation of the manuscript.

Competing Interests: The authors have declared that no competing interests exist.

* E-mail: jain@physics.du.ac.in

Introduction

One of the puzzles in the origin of life is the question: How did large molecules, which are essential for all cells to function, first arise? Macromolecules such as RNA and protein molecules, which contain from about a hundred to several thousand monomers, are produced in cells with the help of two crucial catalysts (a) the RNA polymerase which reads the genes on DNA molecules and produces the corresponding messenger RNA molecules and (b) the ribosome which reads the messenger RNA molecules and produces the corresponding protein molecules. These two powerful catalysts, RNA polymerase and ribosome, are themselves made up of proteins and RNA molecules, each of which is produced by the process mentioned above. When cells produce daughter cells, the latter are already endowed with these catalysts at birth, from which they synthesize other molecules. Nowhere in the living world is there a natural process we know of that produces macromolecules and that does *not* itself use macromolecules. Hence the puzzle. We expect that the answer to the question lies in the processes that occurred before life originated.

The Miller experiment [1] and subsequent work [2–5] were successful in synthesizing monomer building blocks of large molecules in simulated prebiotic environments. Those experiments

suggested that amino acids and nucleotides, monomer building blocks of macromolecules, could be produced on the prebiotic earth. Subsequently there has been much experimental work to explore mechanisms that could enhance the concentrations of monomers and synthesize long polymers [6–9]. While there is interesting progress, as yet there is no compelling scenario for the primordial origin of large molecules.

Meanwhile what has been observed is that catalysis is a fairly ubiquitous property that arises in different kinds of molecules and even at small sizes. Organocatalysts [10–12], peptides [13,14], and RNA molecules [15–17] are known to have catalytic properties. Cofactors play an important role in catalyzing metabolic reactions and they (or their evolutionary predecessors) may have had a role in prebiotic catalysis [18].

The ubiquity of catalysis motivates the main idea behind the present paper. Here we attempt to investigate theoretically, using a mathematical model, whether one can construct a chemical organization that produces large molecules from small ones, using the property of catalysis. Apart from the specific question of the origin of large molecules the present work is also motivated by a larger question of how complex structures and organizations are built incrementally from simpler ones. In systems where catalysis is possible an important self-organizing structure that can appear is

an autocatalytic set (ACS). ACSs were proposed by Eigen [19], Kauffman [20] and Rossler [21] and have been used by many authors to study various aspects of self-organization, evolution and the origin of metabolism [22–31], the origin of replication [32–34], and the origin and dynamics of protocells [35–38]. In order to separate the issues, the present model only has catalysis and no replication or spatial enclosures; we wish to see what can be achieved by catalysis alone.

Farmer et al [22], Bagley et al [39], and Bagley and Farmer [23] proposed and analyzed a model of an artificial chemistry in which polymers could form by ligation of shorter polymers through spontaneous reactions as well as reactions catalyzed by other polymers in the chemistry. Bagley and Farmer [23] analyzed the population dynamics of the molecular species and established some important properties of autocatalytic self-organization. When the food set (monomers) were supplied at a fixed input rate and the chemistry contained an ACS they showed that in a suitable range of parameters the concentrations of the ACS molecules dominated over the rest of the molecules (the background), thereby focusing the chemical resources of the system into a small subset of molecules comprising the ACS. However the largest polymers in the ACSs they considered had about 15–20 monomers; they did not systematically investigate the problems that arise in generating much larger molecules in their chemistry.

These problems were sharply articulated in the work of Ohtsuki and Nowak [34], in which they considered a much simpler model that could be analytically solved. In this model, which they refer to as ‘symmetric prelife’ with a catalyst, they showed that in order for the catalyst to acquire a significant concentration in a prebiotic scenario its catalytic strength should be very large, growing exponentially with its length. The inference from the model, therefore, was that it is difficult for a large catalyst molecule to arise in a prebiotic scenario.

In this work we consider a model of artificial chemistry similar in structure to that of Bagley and Farmer. This model is intermediate in complexity and realism between the model of Bagley and Farmer (which is slightly more complex) and model of Ohtsuki and Nowak (which is much simpler). We study the dynamics of this model in the presence of ACSs and in particular a structure that we refer to as a ‘nested ACS’ in which a small ACS helps trigger a larger one. We show that this mechanism when iterated across a cascade of nested ACSs avoids the problem of exponentially growing catalyst strengths. This mechanism, therefore, provides a possible route to the construction of large molecules in a pre-biotic scenario. Apart from these results our work provides an insight, based on the analytic treatment of the system under certain approximations as well as numerical work, of certain ACS properties and questions such as why ACSs dominate, why nested ACSs work, etc.

Results

The Model

The model is specified by describing the set of molecular species, their reactions, and the dynamical rate equations for their population dynamics. A special set of molecules, the ‘food set’, denoted \mathcal{F} , consists of small molecular species, f in number, that are presumed to be abundantly present in a prebiotic niche. The simplest version of the model ($f=1$) contains only a single monomer species A (or $A(1)$) whose concentration x_1 in a well stirred prebiotic region will be assumed to be buffered (constant). The other molecules, $A(2)$, $A(3)$,... (dimers, trimers, etc.), whose concentrations are denoted x_2, x_3, \dots , are all made through

ligation and cleavage reactions of the type $A(i) + A(j) \rightleftharpoons A(i+j)$ with forward (ligation) rate constant denoted k_{ij}^F and reverse (cleavage) rate constant k_{ij}^R . The net forward flux of this reaction pair is given by $v_{ij} = (k_{ij}^F x_i x_j - k_{ij}^R x_{i+j})$. The rate equations for the system are given by $\dot{x}_1 = 0$, and, for $n=2, 3, \dots$,

$$\begin{aligned} \dot{x}_n &= \sum_{i \leq j, i+j=n} v_{ij} - \sum_{i=1, i \neq n}^{\infty} v_{in} - \phi_n x_n \quad (1) \\ &= \sum_{i \leq j, i+j=n} (k_{ij}^F x_i x_j - k_{ij}^R x_n) + \sum_{i=1, i \neq n}^{\infty} (k_{im}^R x_{i+n} - k_{im}^F x_i x_n) \\ &\quad + 2(k_{mn}^R x_{2n} - k_{mn}^F x_n^2) - \phi_n x_n, \quad (2) \end{aligned}$$

where ϕ_n represents a loss rate of species n from the region in question. The two terms in the first sum represent the formation (respectively, cleavage) of $A(n)$ from (into) smaller molecules. The two terms in the second sum and the following bracket represent the cleavage (respectively, formation) of larger molecules via reactions that produce (consume) $A(n)$. The stoichiometric factor of 2 before the bracket arises because two molecules of $A(n)$ are involved in the corresponding reaction pair. The set of parameters k_{ij}^F , k_{ij}^R that are non-zero define the set of possible reactions; collectively they define the ‘spontaneous chemistry’ (‘spontaneous’ in the sense that the reactions are possible even in the absence of catalysts). A pair of ligation and cleavage reactions can be excluded from the chemistry by setting both k_{ij}^F and k_{ij}^R to zero. The scheme permits chemistries in which some reactions proceed in only one direction (ligation or cleavage) by setting only one of k_{ij}^F and k_{ij}^R to zero. However, we will primarily be interested in a chemistry in which each reaction is reversible. The existence of the cleavage reactions makes it more difficult for the long molecules to survive; thus it is more significant to demonstrate the appearance of long molecules in a model in which cleavage reactions are permitted than in one where only the forward (ligation) reactions are.

We consider a simple scheme for catalyzed reactions, assuming that a molecule enhances the rate of a reaction that it catalyzes in proportion to its own concentration. Thus, if $A(m)$ is a catalyst of the reaction pair $A(i) + A(j) \rightleftharpoons A(i+j)$, then the rate constants of this reaction pair, k_{ij}^F and k_{ij}^R , are replaced $k_{ij}^F \rightarrow k_{ij}^F(1 + \kappa_m^{ij} x_m)$ and $k_{ij}^R \rightarrow k_{ij}^R(1 + \kappa_m^{ij} x_m)$, where κ_m^{ij} is the ‘catalytic strength’ of the catalyst for this reaction pair. The first term in the bracket, unity, represents the spontaneous reaction rate (which is present irrespective of whether the reaction is catalyzed or not), and the second term $\kappa_m^{ij} x_m$ represents the enhancement of the reaction rate due to the catalyst. Note that in this scheme a catalyst enhances both the forward and reverse reaction rates by the same factor. If a reaction has multiple catalysts, $\kappa_m^{ij} x_m$ is replaced by $\sum_m \kappa_m^{ij} x_m$, where the sum runs over all catalysts $A(m)$ of the reaction in question. Typically, only a small subset of the spontaneous reactions will be catalyzed. The set of catalyzed reactions together with the catalysts and their catalytic strengths will be referred to as the ‘catalyzed chemistry’.

When there are f food set (or ‘monomer’) species a general molecule A is represented as an f -tuple of non-negative integers: $A = (i_1, i_2, \dots, i_f)$, where i_l is number of monomers of type l contained in A . The identity of a molecule in the model is completely determined by the number of monomers of each type contained in the molecule; the order in which they appear is irrelevant. Thus the combinatorial diversity of distinct compounds

containing a total of n monomers (of all types) grows only as a power of n ($\sim n^{f-1}$) instead of exponentially ($\sim f^n$ for strings) if the order had mattered. This simplification helps in picturizing the chemistry and significantly reducing the computational power needed to explore large values of n . The reaction scheme and rate equations are similar to the ‘1-dimensional’ version above. Details of the general model and explicit examples of rate equations for $f=1$ and 2 are discussed in the Appendix S1.

The main differences between the present model and that of Bagley and Farmer are (a) a simpler representation of molecules (we do not consider molecules as strings), (b) a simpler treatment of catalysis (we do not consider intermediate complexes), and (c) we ignore the effects coming from small populations containing a discrete number of molecules. We reproduce the main phenomenon of ACS dominance that Bagley and Farmer observed, but the relative simplicity of the present model allows us to explore other phenomena that they do not report about (this includes a multistability in the dynamics and the possibility of building large molecules through nested ACSs).

The main differences with the model of Ohtsuki and Nowak are (a) a much richer spontaneous chemistry of ligation reactions and the inclusion of reverse reactions (which makes an analytical treatment more difficult), and (b) a much more general class of catalyzed chemistries, instead of a single catalyst (which allows us to talk of nested ACSs, in particular). With a specific choice of parameters our $f=1$ model reduces exactly to their ‘symmetric prelife’ model with a catalyst. In spite of greater complexity we are able to numerically reproduce their main results in a much more general setting, and also provide approximate analytical understanding of the results.

Autocatalytic Sets (ACSs). The dynamics of the above system is particularly interesting when ACSs are present in the catalyzed chemistry. Consider a set S of catalyzed one-way reactions. ‘One-way’ means that each reaction in S is either a ligation or cleavage reaction. Thus the set of reactants and the set of products are unambiguously defined for each reaction and the two sets are distinguished. The presence of a given ligation or cleavage reaction in S does not mean that its reverse is also necessarily a member of S . Let $P(S)$ be the union of sets of products of all reactions in S , and $R(S)$ the union of sets of reactants of all reactions in S . We exclude the food set molecules from both $P(S)$ and $R(S)$. We will refer to the set S of catalyzed reactions as an ACS if (a) $P(S)$ includes a catalyst for every reaction in S , and (b) $R(S) \subset P(S)$. The latter condition implies that all members of $R(S)$ can be produced from the food set by (recursively) applying reactions from within S . An ACS thus ensures the existence of a catalyzed pathway, starting from the food set, for the production of each of its products [19–21]. Alternative valid definitions of an ACS can be given (see [40,41] for one such); the above definition suffices for our present purposes and we hope to return to consequences of other kinds of ACSs in the future. Note that if S is an ACS, then its extension, S' , that additionally includes the reverse of some reactions in S , is also trivially an ACS, as in our scheme a catalyst works for both forward and reverse reactions if both exist in the chemistry.

Spontaneous (uncatalyzed) chemistries

Nomenclature. We first consider the case when none of the reactions is catalyzed, $\kappa_m^{ij}=0$ for all ij pairs. For concreteness we first consider spontaneous chemistries that are ‘reversible’, ‘homogeneous’ and ‘fully connected’. A ‘reversible’ chemistry is one for which each allowed reaction is reversible, i.e., $k_{ij}^F \neq 0 \Leftrightarrow k_{ij}^R \neq 0$. A ‘homogeneous’ chemistry is one in which all the nonzero rate constants are independent of the species labels:

$\phi_n = \phi$ for all n , $k_{ij}^F \neq 0 \Rightarrow k_{ij}^F = k_f$ independent of i and j , and $k_{ij}^R \neq 0 \Rightarrow k_{ij}^R = k_r$ independent of i and j . A ‘fully connected’ chemistry is one in which all possible ligation and cleavage reactions are allowed: $k_{ij}^F \neq 0$ and $k_{ij}^R \neq 0$ for all i, j . A chemistry is ‘connected’ if every molecule can be produced from the food set in some pathway consisting of a sequence of allowed reactions. In this paper we discuss spontaneous chemistries that are reversible and homogeneous. We have checked that introducing irreversible reactions and bringing in a small amount of heterogeneity does not change the conclusions. Some results for sparse chemistries are discussed later. For homogeneous and fully connected chemistries the model has 4 parameters, k_f , k_r , ϕ , and the concentration of the monomer, $x_1 \equiv A$.

We explore the model numerically and, to a limited extent, analytically. While the chemistry under consideration is infinite, numerical simulations were done by choosing a finite number N for the size of the largest molecule in the simulation. In simulating Eq. (1) all terms corresponding to reactions in which any molecule larger than $A(N)$ is produced or consumed were omitted. In principle this introduces another parameter, N , an artifact of the simulation. However, one expects that most properties of physical interest should become independent of N when N is sufficiently large. Evidence for this is presented in Appendix S2. Our numerical solution of differential equations was mostly done using the CVODE solver library of the SUNDIALS (Suite of Nonlinear and Differential/Algebraic Equation Solvers) package [42], and, for smaller N values, using XPPAUT [43]. Steady states obtained were verified using numerical root finders in Octave [44] and Mathematica [45].

Steady state properties of the spontaneous chemistry: Populations decline exponentially with the size of molecules. Starting from the initial condition in which all concentrations other than the food set are zero (we refer to this as the standard initial condition), the concentrations were found to increase monotonically and reach a steady state (Fig. 1A). Numerically the graph of steady state x_n versus n on a semi-log plot was found to be approximately a straight line for large n , consistent with the expression

$$x_n = c\Lambda^n = ce^{-\gamma n}, \quad (3)$$

where, c and $\Lambda = e^{-\gamma}$ are constants. Λ , determined by numerically fitting the slope, decreases monotonically as ϕ increases (Fig. 1B).

For $\phi=0$, the following exact analytical solution for the steady state concentrations exists for homogeneous and connected uncatalyzed chemistries:

$$x_n = A \left(\frac{k_f A}{k_r} \right)^{n-1}. \quad (4)$$

To see that this is a fixed point, note that when Eq. (4) holds, then $v_{ij} = k_f x_i x_j - k_r x_{i+j} = 0$ for all $i, j = 1, 2, \dots$; hence the r.h.s. of Eq. (1) vanishes (at $\phi=0$). Thus $\Lambda(\phi=0) = k_f A / k_r$. Hence, whenever $k_f A < k_r$, the steady state concentrations of large molecules are exponentially damped, $\Lambda < 1$.

When $\phi > 0$ we do not have an analytic solution. Numerically, we find that $\Lambda(\phi > 0)$ drops to below 1 even when $\frac{k_f A}{k_r} > 1$. Λ is found to be a monotonically increasing function of k_f and A , and a monotonically decreasing function of k_r and ϕ . This corresponds to the intuition that an increased ligation rate favours large molecules and an increased cleavage or dissipation rate disfavors them. By casting the rate equation in terms of dimensionless variables one can easily see that there are only two independent

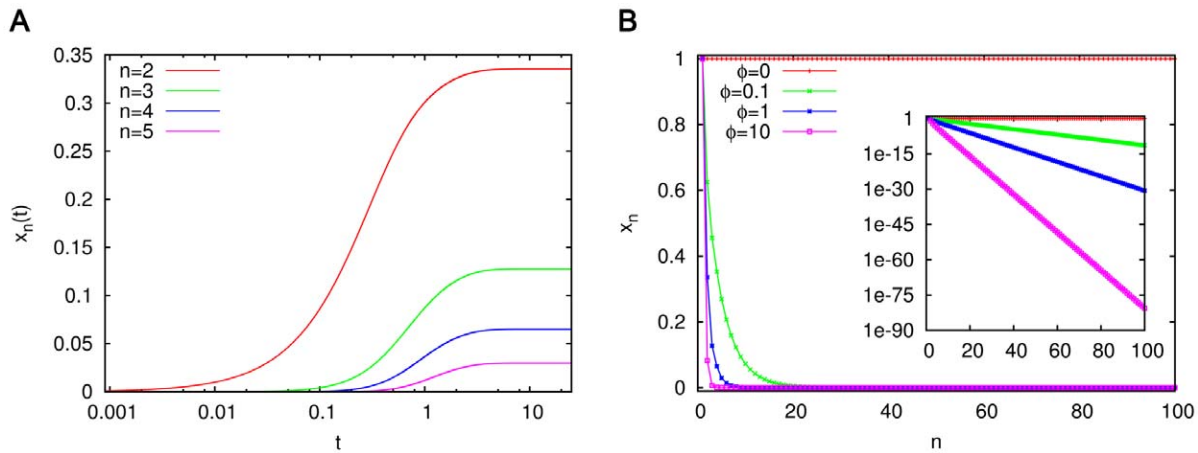


Figure 1. Concentrations in uncatalyzed chemistries with a single food source. (A) Evolution of concentrations with time for a chemistry with $k_f = k_r = A = \phi = 1$. For simulation purposes, the size of the largest molecule was taken to be $N = 100$. (B) Steady state concentration as a function of molecule size. Parameters take the same values as in (A) except that four values of ϕ are shown, $\phi = 0, 0.1, 1, 10$. Inset shows the same on a semi-log plot; the straight lines are evidence of exponential damping of x_n for large n (Eq. (3)), with $\Lambda = 1, 0.77, 0.49, 0.16$ for the four cases, respectively. Λ is computed from the slope of a straight line fit after ignoring the smaller molecules (up to $n = 4$ in this case). doi:10.1371/journal.pone.0029546.g001

parameters, which may be taken to be $k' = k_f A / k_r$ and $\phi' = \phi / k_r$ whenever $k_r \neq 0$ (for details see Appendix S3). Alternatively when $\phi \neq 0$, we can take the two dimensionless parameters to be $\frac{k_f A}{\phi}$ and $\frac{k_r}{\phi}$. The dependence of Λ on these two sets of parameters is also shown in Appendix S3. The uncatalyzed chemistry seems to have a global fixed point attractor (all initial conditions tested lead to the same steady state).

Similar results hold when two food sources are present in the system ($f = 2$) with buffered concentrations of the monomers (1,0) and (0,1). Simulations are done with all possible reaction and cleavage reactions allowed between molecules containing a maximum of N monomers, all with the same forward rate constant k_f and reverse rate constant k_r and a common dissipation rate ϕ for the molecules. A steady state concentration profile is shown in Fig. 2. ‘Diagonal entries’ ($n_1 = n_2$) have higher concentrations in homogeneous chemistries because there are more reaction pathways to build molecules with equal numbers of both monomers than unequal. Since the number of species goes as $N^2/2$ and the number of reactions as $\sim N^4$, computational

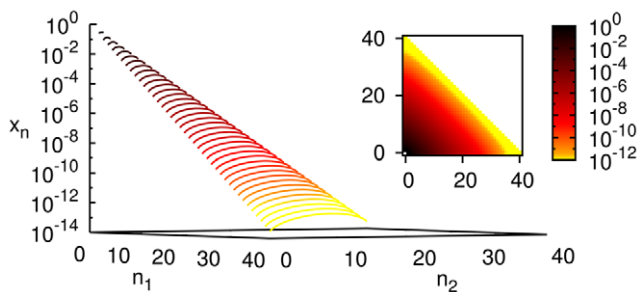
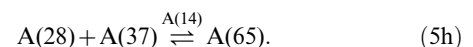
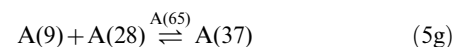
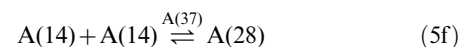
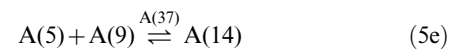
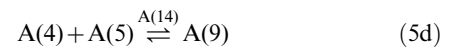
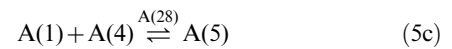
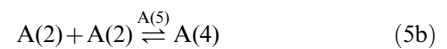
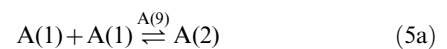


Figure 2. Steady state concentration profile in an uncatalyzed chemistry with $f = 2$. The 3D plot shows the concentration x_n of the molecule $n = (n_1, n_2)$ as a function of n_1 and n_2 in the steady state, for an uncatalyzed chemistry with $k_f = k_r = x_{(1,0)} = x_{(0,1)} = \phi = 1$, $N = 40$. The inset shows a ‘top view’ of the (n_1, n_2) plane with x_n indicated in a colour map on a logarithmic scale. doi:10.1371/journal.pone.0029546.g002

limitations require us to work with a smaller N than for $f = 1$. Qualitative conclusions nevertheless appear to be N independent.

Chemistries with autocatalytic sets

ACS molecules dominate the population in certain parameter regions. We now consider chemistries which contain some catalyzed reactions in addition to the spontaneous reactions described above. As a specific example to display certain generic properties, we consider the catalyzed chemistry defined by equations (5) below and represented pictorially in Fig. 3:



Note that this set of reactions constitutes an ACS (which we will refer to as ACS65). If any one reaction pair is deleted from the set,

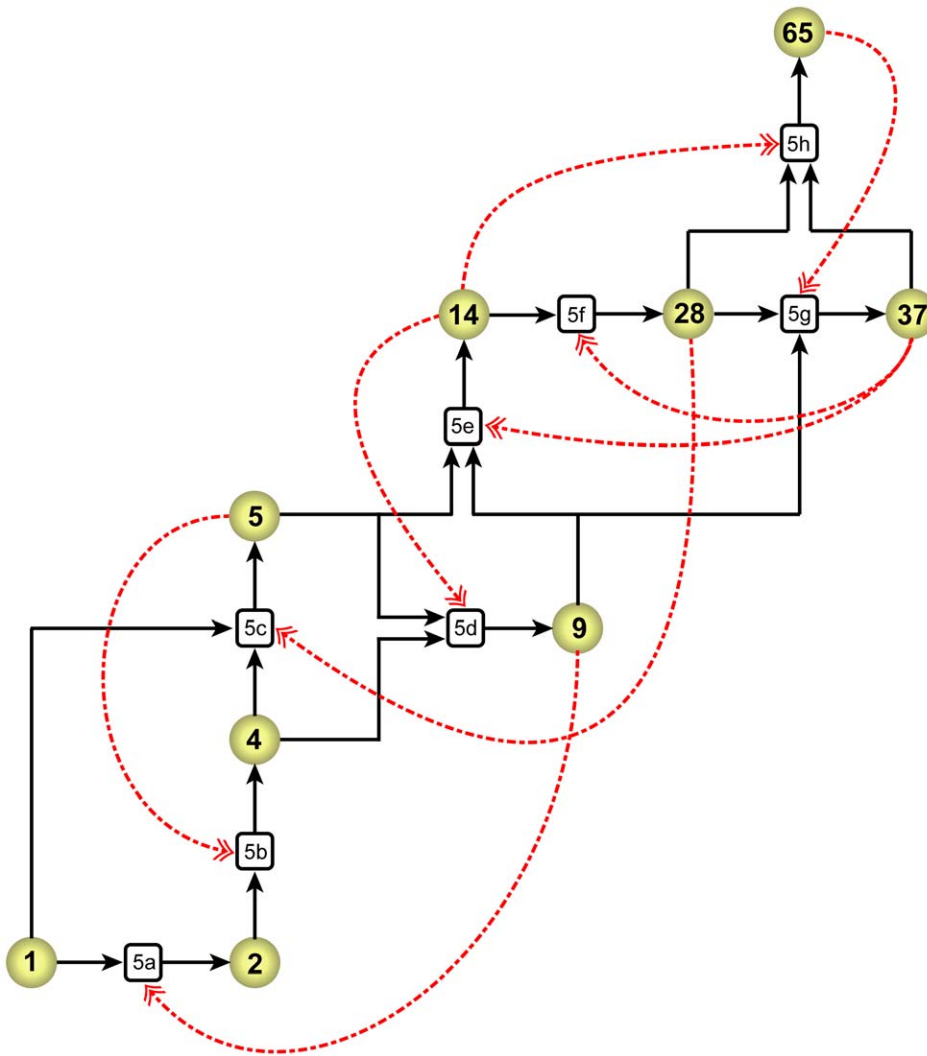


Figure 3. Pictorial representation of the catalyzed chemistry in Eqs. (5), referred to as ACS65. This is a directed bipartite graph with two types of links. Circular nodes represent molecules and rectangular nodes represent reactions. The numbers inside the nodes identify the nodes (molecule size n for circular nodes and reaction equation number for rectangular nodes). A black solid arrow from a molecule to a reaction node indicates that the former is a reactant in the latter, and one from a reaction to a molecule node that the latter is a product of the former. A red dashed arrow from a molecule to a reaction node indicates that the former is a catalyst for the latter. To avoid visual clutter some black arrows starting from molecule nodes are shown to branch out into more than one arrow. (For example, the arrow from molecule node 5 branches into reaction nodes 5d and 5e; this means that molecule 5 is a reactant in both reactions. This structure should not be construed as a bi-directional link between reaction nodes 5d and 5e.) The figure only represents the ligation reactions in the catalyzed chemistry; the reverse (cleavage) reactions are not shown. doi:10.1371/journal.pone.0029546.g003

it is no longer an ACS. For the moment, for simplicity, we consider the case where the catalytic strengths of all the catalyzed reactions are equal ('homogeneous' catalytic strengths): $\kappa_9^{1,1} = \kappa_5^{2,2} = \kappa_{28}^{1,4} = \kappa_{14}^{4,5} = \kappa_{37}^{5,9} = \kappa_{37}^{14,14} = \kappa_{65}^{9,28} = \kappa_{14}^{28,37} = \kappa$, and all other $\kappa_m^{ij} = 0$. (For clarity, in view of double digit indices, we have introduced a comma between the pair of indices in the superscript.) Fig. 4A describes the steady state concentrations, starting from the standard initial condition, for the chemistry that contains these eight catalyzed reactions in addition to all the reactions of the fully connected spontaneous chemistry. At $\kappa = 2.5 \times 10^6$ the ACS product molecules dominate over the background (the 'background' being defined as the set of all molecules except the ACS product molecules and the food set), in the sense that the ACS molecules have significantly larger populations than the background molecules of similar size [23].

There is a fairly sharp threshold value of κ above which ACS domination appears, as evident from the comparison with the lower curve in Fig. 4A drawn for $\kappa = 2.0 \times 10^6$. Fig. 4B shows that the steady state background concentrations decline as ϕ increases, while the ACS concentrations are relatively unaffected in this regime (thus ACS domination increases). If catalyzed production pathways from the food set to other molecules are broken somewhere, the concentration of the latter molecules declines significantly. This is evident from Fig. 4C for which only one reaction pair (5) is deleted from the catalyzed chemistry (which now contains no ACS) while others are catalyzed at the same strength as before.

ACS domination at a sufficiently high catalytic strength also occurs when there is more than one monomer. An example with $f = 2$ is shown in Fig. 5 whose list of catalyzed reactions is given in Table S1.

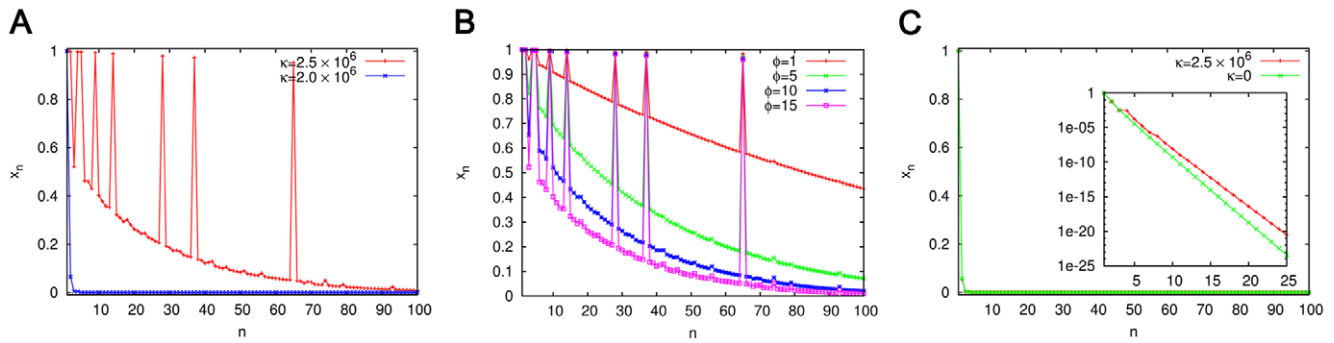


Figure 4. Steady state concentration profile for ACS65 (Eqs. (5)). In all the cases $k_f = k_r = A = 1$, $N = 100$. (A) The concentration profile for two values of κ for $\phi = 15$. (B) The concentration profile for four values of ϕ for $\kappa = 3.0 \times 10^6$. (C) The concentration profile for $\kappa = 2.5 \times 10^6$, $\phi = 15$ but with reaction (5a) removed from the ACS (red curve) compared with the profile for the spontaneous chemistry, $\kappa = 0$, $\phi = 15$ (green curve). The inset shows the same with x_n on a logarithmic scale. On the linear scale the two curves are indistinguishable. doi:10.1371/journal.pone.0029546.g004

Understanding why ACS concentrations are large (the $\kappa \rightarrow \infty$ limit). The above features are generic for a large class of ACSs. It is instructive to consider the $\kappa \rightarrow \infty$ limit which we discuss analytically. When κ is nonzero, the terms in Eq. (1) corresponding to catalyzed reactions get modified. The net flux v of such reaction pairs on the r.h.s. (for brevity we are omitting the subscript ij in v_{ij}) is replaced by $(1 + \kappa \sum_m x_m)v$, where the sum over m is a sum over all catalysts of the reaction pair. Now let the set S of catalyzed reactions be an ACS. Then, if $A(n) \in P(S)$ the r.h.s. of \dot{x}_n contains at least one such catalyzed term, while if $A(n) \notin P(S)$ \dot{x}_n contains no such term. For example, for ACS65, we have

$$\dot{x}_2 \simeq \kappa(x_9 v_{1,1} - 2x_5 v_{2,2}) + (\text{terms independent of } \kappa) \quad (6a)$$

$$\dot{x}_4 \simeq \kappa(x_5 v_{2,2} - x_{28} v_{1,4} - x_{14} v_{4,5}) + (\kappa^0 \text{ terms}) \quad (6b)$$

$$\dot{x}_5 \simeq \kappa(x_{28} v_{1,4} - x_{14} v_{4,5} - x_{37} v_{5,9}) + (\kappa^0 \text{ terms}) \quad (6c)$$

$$\dot{x}_9 \simeq \kappa(x_{14} v_{4,5} - x_{37} v_{5,9} - x_{65} v_{9,28}) + (\kappa^0 \text{ terms}) \quad (6d)$$

$$\dot{x}_{14} \simeq \kappa(x_{37} v_{5,9} - 2x_{37} v_{14,14}) + (\kappa^0 \text{ terms}) \quad (6e)$$

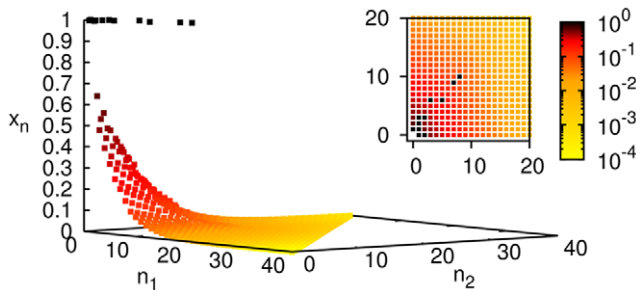


Figure 5. Steady state concentration profile for ACS(8,10) in a chemistry with $f=2$. The convention is same as in Fig. 2. The molecules and reactions of the ACS are given in Table S1, the largest molecule being (8,10). $k_f = k_r = x_{(1,0)} = x_{(0,1)} = 1$, $\phi = 10$, $\kappa = 10^6$, $N = 40$. doi:10.1371/journal.pone.0029546.g005

$$\dot{x}_{28} \simeq \kappa(x_{37} v_{14,14} - x_{65} v_{9,28} - x_{14} v_{28,37}) + (\kappa^0 \text{ terms}) \quad (6f)$$

$$\dot{x}_{37} \simeq \kappa(x_{65} v_{9,28} - x_{14} v_{28,37}) + (\kappa^0 \text{ terms}) \quad (6g)$$

$$\dot{x}_{65} \simeq \kappa(x_{14} v_{28,37}) + (\kappa^0 \text{ terms}), \quad (6h)$$

while the rate equations for all other (non ACS) molecules (\dot{x}_3 , \dot{x}_6 , etc.) have no terms proportional to κ . In a steady state solution the r.h.s. of Eqs. (6) is zero, and to leading order in the $\kappa \rightarrow \infty$ limit we must set the coefficients of κ to zero. The coefficients involve only the ACS fluxes v_{ij} and catalyst concentrations. Each coefficient is a sum of terms, and each term is proportional to an ACS flux v_{ij} . Thus $v_{ij} = 0$ for the ACS fluxes provides a steady state solution in the $\kappa \rightarrow \infty$ limit. Numerically we find that when κ is sufficiently high the rate equations converge to this solution starting from the standard initial condition. Now $v_{ij} = k_f x_i x_j - k_r x_{i+j}$, therefore $v_{ij} = 0$ implies $x_{i+j} = k_f x_i x_j / k_r$ for the members of $P(S)$. Since by definition there is a catalyzed pathway from the food set to every ACS product, we can recursively express the steady state concentration of every ACS molecule in terms of $x_1 = A$: $x_n = A(k_f A / k_r)^{n-1}$.

It is evident that this argument applies whenever the set S of catalyzed reactions is an ACS; thus for every member of $P(S)$, $x_n \simeq A(k_f A / k_r)^{n-1}$ is a steady state solution of the rate equations in the limit $\kappa \rightarrow \infty$. This is corroborated numerically: in Fig. 4B since $A = k_f = k_r = 1$, all the eight ACS products should have $x_n = 1$ in this limit; the numerical result at $\kappa = 3 \times 10^6$ is not too far from this limiting analytical value.

A strong ACS counteracts dissipation. Recall from Eq. (4) and the discussion following it that every molecule in a homogeneous connected uncatalyzed chemistry has the steady state concentration $x_n = A(k_f A / k_r)^{n-1}$ when there is no dilution flux or dissipation ($\phi = 0$), and a smaller concentration when there is dissipation ($\phi > 0$). We have observed above that an ACS with a sufficiently large κ can boost the steady state concentrations of its members, even when $\phi > 0$, to the same level. The expression $x_n = A(k_f A / k_r)^{n-1}$ seems to represent an upper limit on the steady state concentration of $A(n)$, which can be approached either when dissipation goes to zero, or, when there is dissipation, by membership of an ACS whose catalytic strength becomes very large.

When the reaction pair $A(1)+A(1)\rightleftharpoons A(2)$ is not catalyzed the production of $A(2)$ takes place at a much smaller rate, the spontaneous rate. Therefore its concentration is much smaller, and hence so are the concentrations of the larger molecules.

When $A(n)$ belongs to the background the r.h.s. of \dot{x}_n contains no term proportional to κ , and all the κ -independent terms have to be kept, including the ϕx_n term. Thus its steady state concentration depends upon ϕ , and as in the case of the uncatalyzed chemistry, declines more rapidly with n when ϕ increases.

Multistability in the ACS dynamics and ACS domination. The reason for the sudden change in the qualitative character of the steady state profile as κ is increased is a bistability in the chemical dynamics due to the presence of the ACS. Fig. 6 shows three regions in the phase diagram of the system, separated by values κ^I and κ^{II} of κ . For $0 \leq \kappa < \kappa^I$ (region I), the dynamics starting from both the initial conditions mentioned in the figure caption converged to the same attractor configuration, which is a fixed point in which the large ACS molecules have a very small concentration (the concentration declines exponentially with n). For $\kappa^{II} < \kappa$ (region III), again they converge to a single attractor, a fixed point in which the ACS molecules have a significant concentration which approaches $x_n = A(k_f A/k_r)^{n-1}$ as $\kappa \rightarrow \infty$. In the range $\kappa^I \leq \kappa \leq \kappa^{II}$ (region II), they converge to two different stable attractors, both fixed points for the ACS under discussion. (We remark that using other initial conditions we have found at least one more stable fixed point in a part of region II which has intermediate values of x_{65} , indicating that this system has multistability.)

This phase structure implies that if we start from the standard initial condition and consider the steady state profile to which the system converges for different values of κ , we will see a sharp change in the steady state profile as κ is increased from a value slightly below κ^{II} to a value slightly above κ^{II} . Below κ^{II} the large

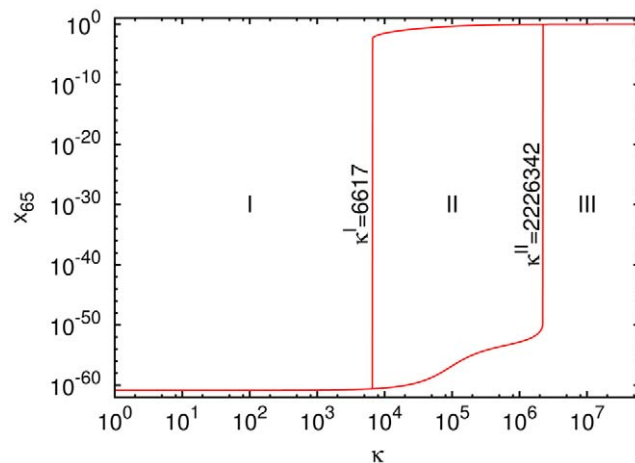
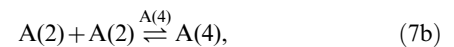
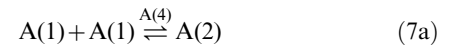


Figure 6. Bistability in the dynamics of ACS65. ‘Hysteresis curve’ of the steady state concentration of $A(65)$ versus κ for $k_f = k_r = A = 1$, $\phi = 15$, $N = 100$. The curve is obtained by using two different initial conditions (i) the standard initial condition $x_n = 0$ for all $n \geq 2$, and (ii) a ‘high’ initial condition $x_n = 1$ for all $n \geq 2$. In region I ($\kappa < \kappa^I = 6617$) both initial conditions lead to a single fixed point in which x_{65} is very low, 10^{-60} . In region III ($\kappa > \kappa^{II} = 2226342$) both initial conditions again lead to a single fixed point but in this fixed point x_{65} is high, close to unity. In region II ($\kappa^I \leq \kappa \leq \kappa^{II}$) the initial condition (i) leads to the lower fixed point and (ii) leads to the upper one. The transitions are very sharp, e.g., at $\kappa = 2226341$ the system is numerically clearly seen in region II and at 2226343 in region III. doi:10.1371/journal.pone.0029546.g006

ACS molecules will be essentially absent in the steady state, and above κ^{II} they will be present in large numbers and will dominate over the background.

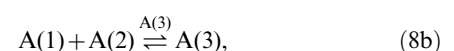
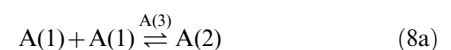
Therefore, following the nomenclature of Ohtsuki and Nowak [34], who observed a similar bistability in their model with a single catalyst, we refer to κ^{II} as the ‘initiation threshold’ of the ACS. Similarly κ^I will be referred to as the ‘maintenance threshold’ of the ACS, because once the ACS has been initiated, κ can come down to as low a value as κ^I , and the ACS will continue to dominate.

Bistability in simple ACSs. In general κ^I and κ^{II} depend upon the other parameters, as well as the topology of the catalyzed and spontaneous chemistries. The phase structure is exhibited in more detail for a simpler example in Fig. 7, where the catalyzed chemistry consists of only two reaction pairs:



which constitute an ACS (called ACS4). This system, investigated numerically using XPPAUT, shows bistability. For a fixed ϕ the bistability diagram is shown in Fig. 7A. The dependence of κ^I, κ^{II} on ϕ is exhibited in Fig. 7B, and on both ϕ and k_f in Fig. 7C. For a given k_f , there is critical value of $\phi (= \bar{\phi})$ at which the κ^I and κ^{II} curves meet, below which there is no bistability. The locations of the phase boundaries, the κ^I and κ^{II} curves, depend upon the specific underlying chemistries (catalyzed and spontaneous) as well as the ACS topology. The steady state profiles are shown at sample points in the phase space in Fig. 7D. For $\phi > \bar{\phi}$ it can be seen, that as in the case of the larger ACS discussed earlier, if we start from the standard initial condition, the largest molecule of the catalyzed chemistry, here $A(4)$, dominates over the background in the steady state only for $\kappa > \kappa^{II}$ (e.g., the panel marked 3 in Fig. 7D). In the range $\kappa^I \leq \kappa \leq \kappa^{II}$, it dominates only if we start from initial conditions where it has a large enough value to begin with (panel 2b), but not if we start from the standard initial condition (panel 2a). It does not dominate for any initial condition if $\kappa < \kappa^I$ (panel 1). If ϕ is below $\bar{\phi}$, there is a single attractor with no significant ACS dominance if κ is small (panel 4), or if κ is large (panel 5), ACS dominance exists but is not very pronounced as the background concentrations are also substantial.

We remark that while bistability seems to be quite generic in homogeneous chemistries containing ACSs, the existence of an ACS does not guarantee that bistability exists somewhere in phase space. For example consider the simplest possible chemistry ($N = 2$) containing only the monomer (which is buffered) and the dimer. If we assume that the sole reaction pair $A(1) + A(1) \rightleftharpoons A(2)$ is catalyzed by $A(2)$, the catalyzed chemistry is trivially an ACS and the only rate equation is $\dot{x}_2 = k_f A^2(1 + \kappa x_2) - k_r x_2(1 + \kappa x_2) - \phi x_2$. The system can be solved exactly and always goes to a global fixed point attractor starting from any initial condition $x_2(0) \geq 0$. However, the $N = 3$ chemistry defined by the two catalyzed reactions



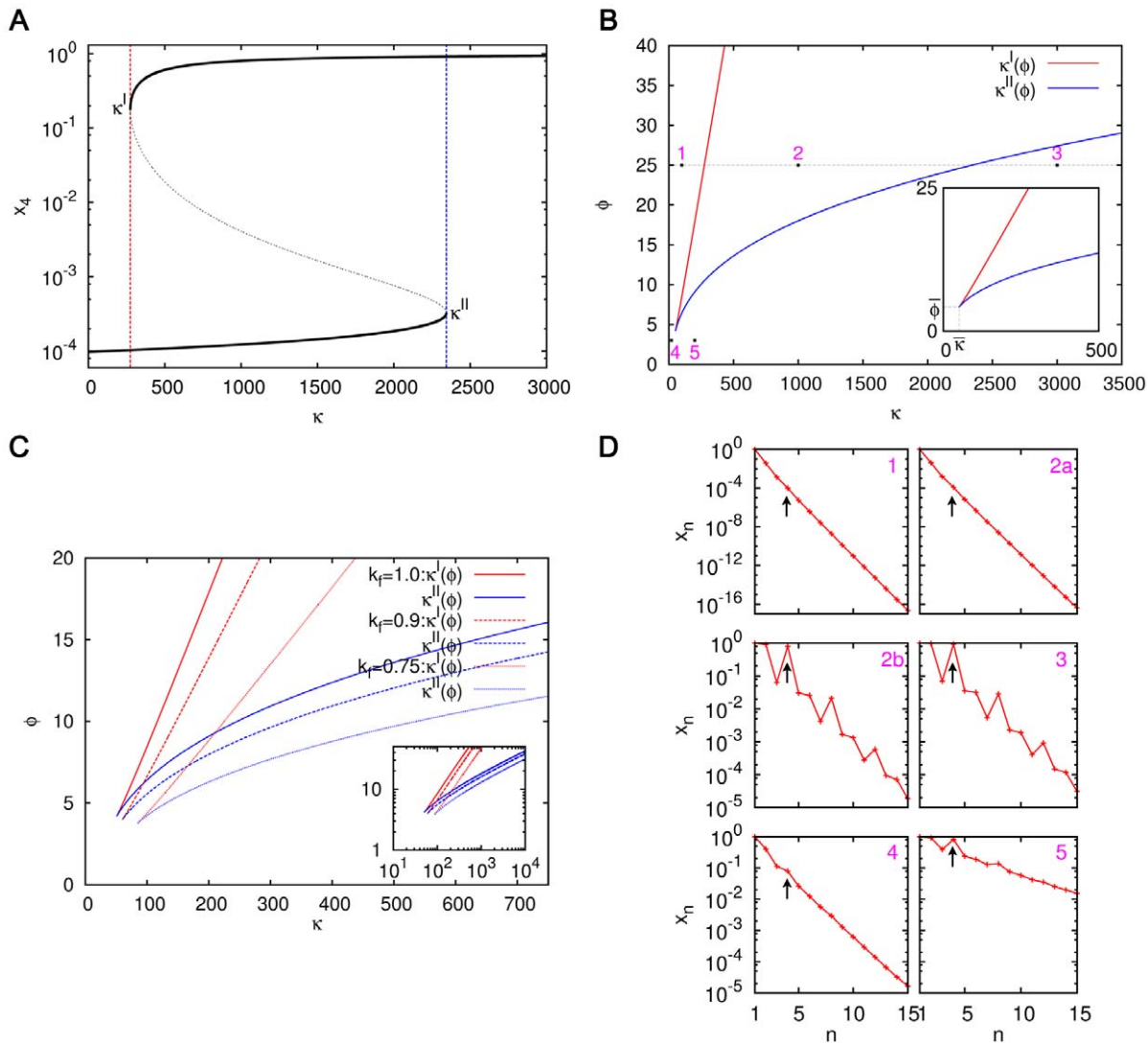


Figure 7. Phase diagram and concentration profiles for ACS4. (A) The steady state concentration x_4 versus κ for $k_f = k_r = A = 1$, $\phi = 25$, $N = 15$. The bistable region exists for the range $\kappa^I \leq \kappa \leq \kappa^{II}$ in which different initial conditions lead to two distinct steady state values of x_4 . The solid black curves correspond to the two stable fixed points, and the dotted black curve to the unstable fixed point. (B) The dependence of κ^I (red curve) and κ^{II} (blue curve) on ϕ for $k_f = k_r = A = 1$, $N = 15$. The bistable region lies between the two curves; in the rest of the phase space the system has a single fixed point. The inset shows the location of the critical point $(\bar{\kappa}, \bar{\phi})$; there is no bistability for $\phi < \bar{\phi}$. (C) Dependence of the phase boundaries on k_f for $k_r = A = 1$, $N = 15$, with the inset showing the behaviour on a log-log plot. (D) The steady state concentration profile of molecules shown at five representative points in the phase space (numbered 1 through 5 and marked in (B)). Note that at the phase point 2 that lies between the κ^I and κ^{II} curves there are two steady state profiles corresponding to the two stable fixed points of the system. The figure marked 2a shows the profile starting from the standard initial condition, and 2b from the initial condition where $x_n = 1$ for all n . The arrows draw attention to the concentration of the catalyst, A(4). doi:10.1371/journal.pone.0029546.g007

does exhibit bistability at a sufficiently large ϕ . Ohtsuki and Nowak [34] had also found a lower limit on catalyst size for bistability to exist in their model. Similar results hold for the $f = 2$ case. From our simulations a general observation seems to be that bistability is ubiquitous at sufficiently large values of ϕ in homogeneous chemistries whenever the smallest catalyst is large enough compared to the food set. When it does exist it seems to provide a crisp criterion for ‘ACS domination’, including ‘initiation’ ($\kappa > \kappa^{II}$) and ‘maintenance’ ($\kappa \geq \kappa^I$).

We must mention that there exists a substantial mathematical literature on the nature of attractors in chemical reaction systems including conditions for multistability and monotonicity [46–50]. It would be interesting to apply some of those results to models of

the kind being studied here, which involve a large number of molecular species.

A problem for primordial ACSs to produce large molecules: The requirement of exponentially large catalytic strength

A natural initial condition for the origin of life scenario is one where only the food set molecules, and perhaps a few other not very large molecules (dimers, trimers, etc.) have nonzero concentrations, while the large molecules have zero concentrations. It is from such an initial condition that we would like to see the emergence of large molecules through the dynamics. We have seen that in uncatalyzed chemistries, the concentrations of the

large molecules remain exponentially small ($x_n \sim e^{-\gamma n}$, $\gamma > 0$). In catalyzed chemistries, especially in the presence of an ACS, a few specific large molecules produced by the ACS can acquire a high population. However, this seems to require a large catalytic strength for the catalysts. For example, for ACS65 this happens at $\kappa > \kappa^H = 2226342$, starting from the standard initial condition. The fact that such a large catalytic strength is needed to produce appreciable concentrations of molecules of even moderate length like $n = 65$ could be a problem for the ACS mechanism to produce large molecules in the kind of prebiotic scenario we are considering. In this section we characterize the problem somewhat more quantitatively by determining how κ^H depends upon the size n of the catalysts in the ACS.

As mentioned earlier, the values of κ^I , κ^H depend on the topology of the ACS. The topology of the ACS includes the set of catalyzed reactions and the assignment of catalysts to each of the catalyzed reactions. Define the ‘length’ L of an ACS as the size of (i.e., the total number of monomers of all types in) the largest molecule produced in the ACS. An ‘extremal’ ACS of length L will be referred to as one in which all reactions belonging to the ACS are catalyzed by the same molecule which is the largest molecule (of size L) in the ACS. For concreteness, since we are interested in the dependence of κ^H on the catalyst size, we consider only extremal ACSs of length L . We assume that the catalyst has the same catalytic strength κ for all the reactions in the ACS. We wish to determine the bistable region for such ACSs and in particular how the values of κ^I and κ^H depend upon L . These values depend upon the precise set of catalyzed reactions constituting the ACS. For illustrative purposes we consider three different ways of generating the ACS described under Methods as Algorithm 1, 2 and 3, which generate ACSs with different characteristic structure.

We determine the κ^I and κ^H values for ACSs of different values of L numerically. These are plotted in Fig. 8. It is evident that κ^I increases with L according to a power law $\kappa^I \sim L^\alpha$ (with α ranging from 2.1 to 2.8 for the three algorithms), while κ^H increases exponentially,

$$\kappa^H \sim e^{\rho L}, \quad (9)$$

with $\rho \approx 0.64$ for all the algorithms. α and ρ depend upon the other parameters. In particular we find that ρ increases with ϕ , i.e., the catalytic strength needed for large molecules to arise increases faster with the size of catalyst at larger values of dissipation. This generalizes, to a much larger class of models, the results of Ohtsuki and Nowak [34], who found a linear dependence of κ^I on L and an exponential dependence of κ^H .

The exponential increase of the initiation threshold, κ^H , with L , quantifies the difficulty in using ACSs to generate large molecules in the primordial scenario of the type modeled above. This means that one needs large molecules with unreasonably high catalytic strengths to exist in the chemistry in order to get them to appear with appreciable concentrations starting from physically reasonable primordial initial conditions.

Nested ACSs: Using a small ACS to reinforce a larger one

We now discuss a mechanism that may overcome the barrier of large catalytic strengths, and may enable large molecules to arise from primordial initial conditions without exponentially increasing catalytic strengths. This mechanism relies on the existence of multiple ACSs of different sizes in the catalyzed chemistry, in a topology such that the smaller ACSs reinforce the larger ones, thereby enabling large molecules to appear with significant concentrations without exponentially increasing their catalytic strength.

To illustrate the basic idea we consider the following simple example where the catalyzed chemistry contains only two ACSs, one of length three and the other of length eight (which we refer to as ACS3 and ACS8, respectively), each generated by the Algorithm 2 mentioned above. All reactions of the former are catalyzed by A(3) with a catalytic strength κ_3 , and of the latter by A(8) with the catalytic strength κ_8 . Thus the two ACSs are:

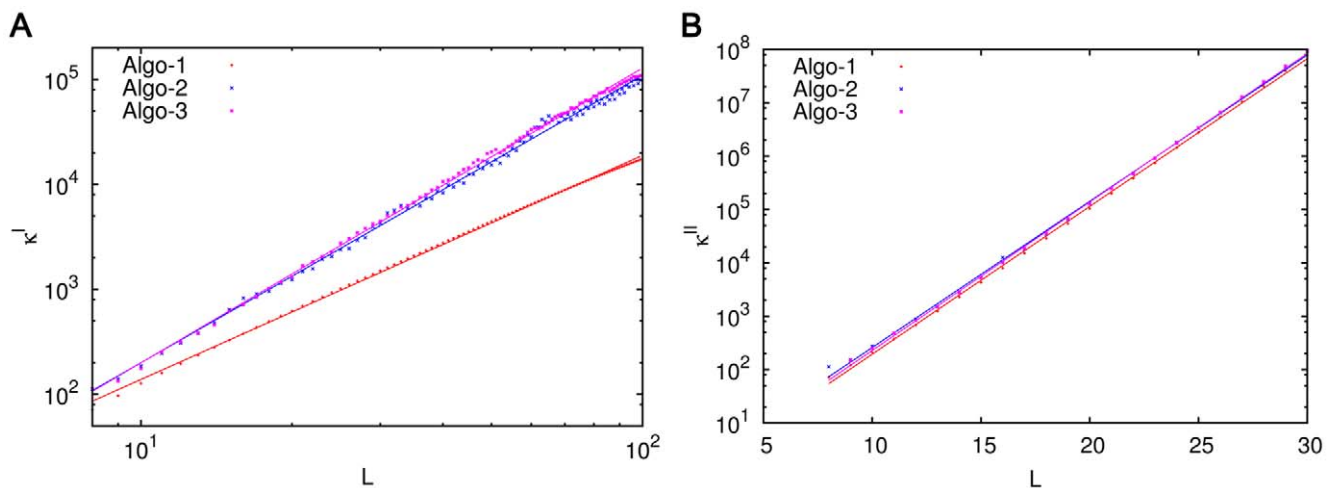
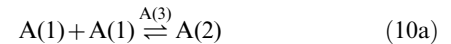
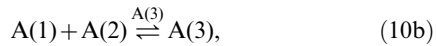
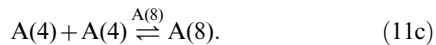
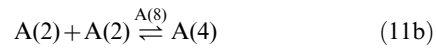
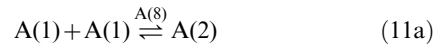


Figure 8. The dependence of the bistable region on catalyst length L . (A) The dependence of κ^I on L . (B) The dependence of κ^H on L . Simulations were done for extremal ACSs of length L generated by three algorithms (see Methods), represented in the figure by different colours. For each L the ACS in question has the property that the largest molecule produced in the ACS has L monomers and catalyzes all the reactions in the ACS. All simulations were done for $k_f = k_r = A = \phi = 1$. $N = 100$ in all cases except the κ^I curve for Algorithm 1, where $N = 200$, because in this case ‘finite- N ’ effects were quite significant at $N = 100$. The figures suggest an approximate power law growth of κ^I and exponential growth of κ^H with L . doi:10.1371/journal.pone.0029546.g008



and



The catalyzed chemistry consists of the above five catalyzed reaction pairs (we will refer to this catalyzed chemistry as ACS3+8). This is pictorially depicted in Fig. 9A. The system also exhibits bistability, and the concentration of A(8) in the two fixed point attractors is exhibited in Fig. 10 as a function of κ_3 and κ_8 .

When κ_3 is small the two pictures in Fig. 10 show the usual bistability of ACS8 along the κ_8 axis. The initiation and maintenance thresholds are $\kappa_8^I = 1.78 \times 10^7$ and $\kappa_8^M = 1145$ given by the location of the boundary between the low concentration region (blue, $x_8 \sim 10^{-7}$) and the high concentration region (yellow $x_8 \sim 1$) along the κ_8 axis in Figs. 10A and 10B respectively. As κ_3 increases, the initiation threshold of ACS8 decreases slowly for a while, then drops sharply near $\kappa_3 = 141$. This value of κ_3 is the initiation threshold of ACS3 when $\kappa_8 = 0$. When κ_3 exceeds this value, the steady state value of x_8 is either high (yellow, $x_8 \sim 1$) or intermediate (orange, $x_8 \sim 10^{-3}$), depending upon the value of κ_8 .

The key point is that the initiation threshold of the larger catalyst depends on the catalytic strength of the smaller catalyst.

The former plummets sharply when the latter approaches the initiation threshold of the smaller catalyst, dropping to a much lower value than before (compare the lower limit of the yellow region in Fig. 10A to the left and right of $\kappa_3 = \kappa_3^I = 141$; the value of κ_8^I plunges several orders of magnitude from 1.78×10^7 at $\kappa_3 = 0$ down to 2178 at $\kappa_3 = 141$). Starting from the standard initial condition, thus, the larger catalyst can acquire a significant concentration at a much lower value of its catalytic strength in the presence of a smaller ACS operating above its initiation threshold than in its absence.

Why a small ACS reinforces a larger one

We now present an intuitive explanation of the above mentioned property. The argument rests on two observations.

(a) **Why the initiation threshold is exponentially large.** The first observation attempts to explain why κ^I is so large in the first place. The contribution of a catalyst to the rate of the reaction it catalyzes appears through the factor $1 + \kappa x$, where κ is the catalytic strength of the catalyst and x its concentration. The term unity in the above factor is the relative contribution of the spontaneous (uncatalyzed) reaction rate. If the catalyst is to play a significant role in the reaction, the catalytic contribution to the reaction rate should be at least comparable to the spontaneous rate, i.e., κx should be at least comparable to unity. As we have seen earlier the concentration of large molecules is typically damped exponentially with their size. Therefore the compensating factor κ needs to increase exponentially in order for the catalyzed reaction rate to be comparable to the spontaneous reaction rate. For concreteness consider the extremal ACSs of length L and consider the steady state population x_L of the catalyst A(L) in the low fixed point as κ is increased. In the spirit of this rough argument one expects that at the initiation threshold the term $\kappa^I x_L$ should be of order unity. In Fig. 11 we display this product for different values of L . Though there is a secular decreasing

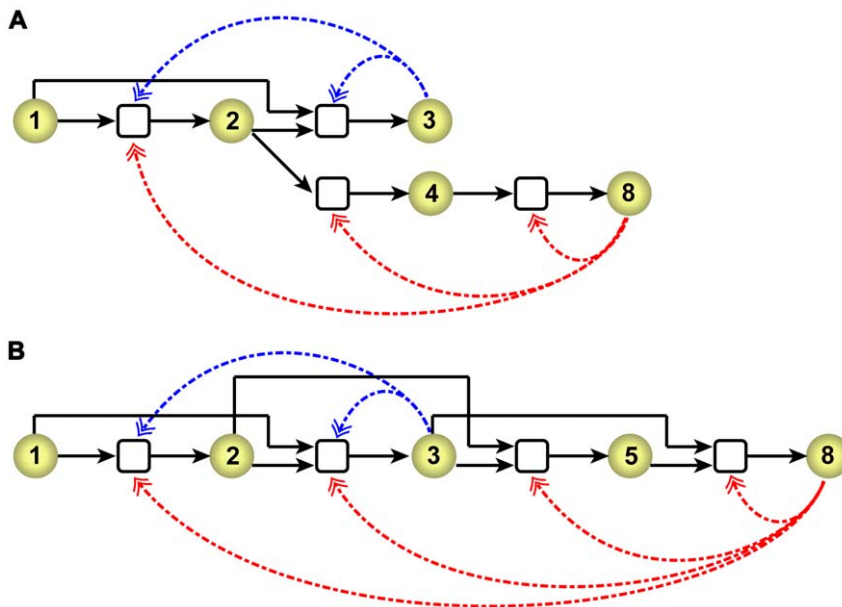


Figure 9. Pictorial representation of nested ACSs. (A) ACS3+8, defined by Eqs. (10) and (11). (B) ACS3+8', defined by Eqs. (10) and (12). The notation is the same as for Fig. 3. The dashed arrows (catalytic links) are given in two colours, blue and red, to distinguish the two ACSs whose catalysts are molecules A(3) and A(8), respectively. Reactions having two catalysts are given by two distinct equations in the text (e.g. (10a) and (11a)), but in the figure are represented by a single reaction node with two incoming catalytic links (the reaction node is not duplicated to avoid visual clutter).

doi:10.1371/journal.pone.0029546.g009

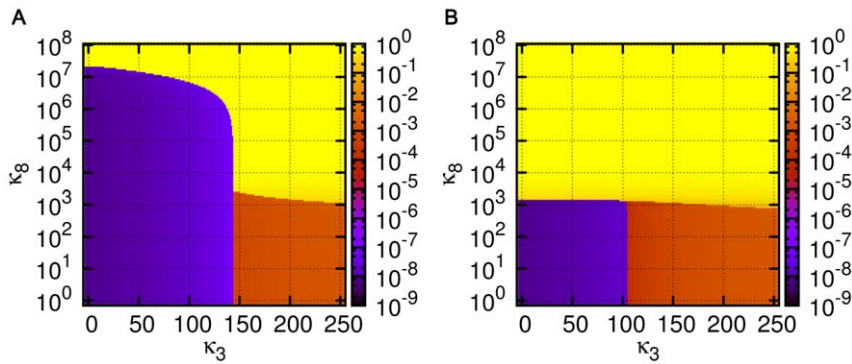


Figure 10. Reinforcement of a larger ACS by a smaller one: The case of ACS3+8. The figure shows the steady state concentration x_8 (in colour coding as indicated) for two different initial conditions as a function of κ_3 and κ_8 , the catalytic strengths of A(3) and A(8) respectively. All simulations were done for $k_f = k_r = A = 1$, $\phi = 20$, $N = 100$. The two figures (A) and (B) differ in the initial condition of the dynamics. (A) The standard initial condition, (B) initial condition $x_n = 1$ for all $n = 2, 3, \dots, N$. doi:10.1371/journal.pone.0029546.g010

trend with L , this product remains of order unity (Fig. 11A) even as the individual factors change over several orders of magnitude (Fig. 11B). This lends numerical support to the above explanation for the exponential dependence of κ^{II} on L .

(b) **Role of the background and spontaneous reactions.** The second observation is that when κ exceeds the initiation threshold for a catalyzed chemistry containing an ACS, not only do the steady state concentrations of the ACS product molecules rise by several orders of magnitude, but also those of the background molecules rise. As an example compare the two steady state profiles of ACS65 in Fig. 4A, which correspond to values of κ below and above the initiation threshold. As one goes from the lower to the upper curve, the concentration of the ACS members of course increases dramatically (as shown by the sharp peaks), but note that the concentrations of other molecules not produced by catalyzed reactions also goes up significantly. Thus in the chemistry containing two ACSs (ACS3+8) as one moves along the κ_3 axis in Fig. 10A and crosses the initiation threshold of ACS3 (i.e., κ_3 exceeds $\kappa_3^{II} = 141$), the concentration of A(8) (a molecule

belonging to the background of ACS3 as its production is not catalysed by ACS3) increases from $\sim 10^{-7}$ (blue region) to $\sim 10^{-3}$ (orange region). This increase in the concentration of A(8) by a factor of $\sim 10^4$ makes it easier for ACS8 to function and its initiation threshold drops by a corresponding factor of about 10^4 (from $\sim 10^7$ to $\sim 10^3$).

This fact highlights the role of spontaneous reactions in the overall dynamics. The background molecules are connected to the ACS through spontaneous reactions, and if it were not for the latter, an ACS would not be able to push up the concentrations of its nearby background. We shall refer to a structure such as the one described above containing ACSs of different sizes with the smaller ACS feeding into the larger one through the spontaneous reactions as a ‘nested ACS’ structure.

The role of ‘overlapping’ catalyzed pathways in nested ACSs

The above example also serves to highlight some other features of catalyzed chemistries containing multiple ACSs. Note that the

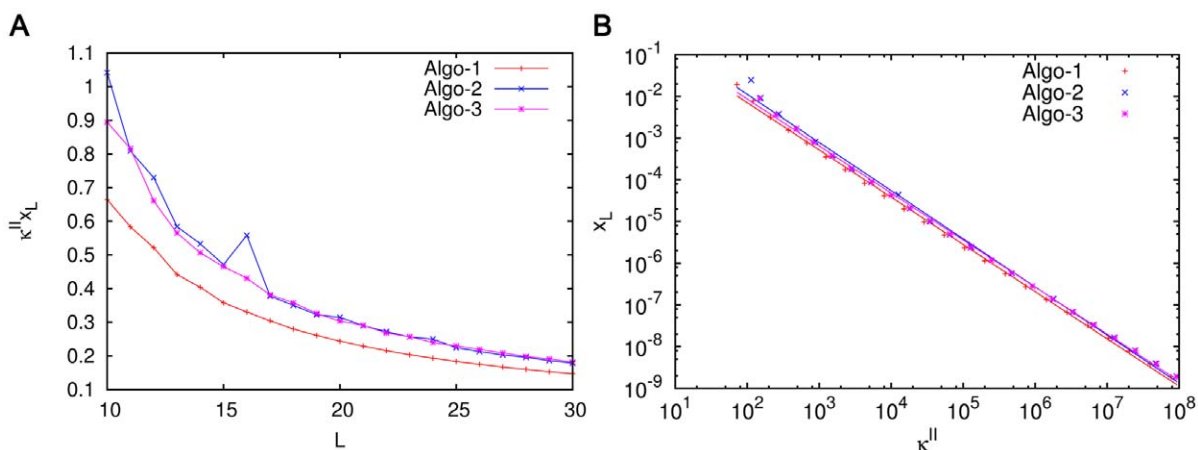
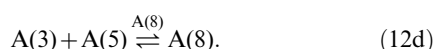
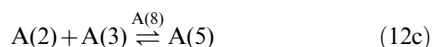
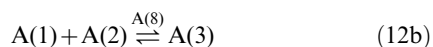
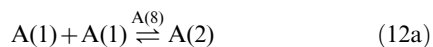


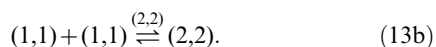
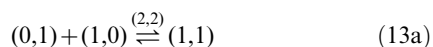
Figure 11. The product $\kappa^{II} x_L$ is of order unity. This figure is produced from the same data as was used for Fig. 8. Simulations were done for chemistries containing extremal ACSs of length L generated by the three algorithms discussed earlier, represented in the figure by different colours. For this figure each chemistry was simulated at a value of κ equal to the initiation threshold κ^{II} corresponding to that chemistry, and the steady state concentration x_L of the catalyst was determined in the low fixed point (starting from the standard initial condition). The parameters values are the same as in Fig. 8. (A) The product of κ^{II} and x_L as a function of L . (B) x_L versus κ^{II} on a log-log plot. The slopes of the fitted straight lines vary in the range -1.13 to -1.16 for the three algorithms (slope $= -1$ would have meant that $\kappa^{II} x_L$ is strictly constant). The figure shows that while each individual factor κ^{II} and x_L ranges over several orders of magnitude, their product, though not constant, is of order unity. doi:10.1371/journal.pone.0029546.g011

production pathway of A(8) in ACS8 (Eqs. 11 and Fig. 9A) contains one reaction pair in common with ACS3, namely the reaction pair $A(1)+A(1)\rightleftharpoons A(2)$. One can consider a situation wherein the overlap is greater. E.g., consider the ACS8' defined by

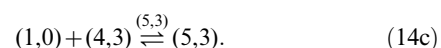
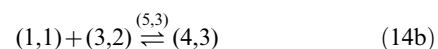
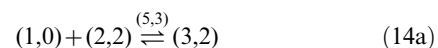


Now the set of reactions in ACS3 is a subset of ACS8' (ignoring the catalyst, which is different in the two cases). The degree of overlap of the catalyzed reaction sets between a pair of nested ACSs makes a difference in the dynamics. Consider, for example, the catalyzed chemistry consisting of ACS3 and ACS8', i.e., the set of catalyzed reactions given by Eqs. (0) and (0), which we refer to as ACS3+8'. This is pictured in Fig. 9B. Like ACS3+8, this chemistry also shows a reduction of κ_8^H , when κ_3 exceeds its initiation threshold. We find that while at $\kappa_3=0$ the value of κ_8^H for the two chemistries is not too different (1.6×10^7 for ACS3+8' versus 1.8×10^7 for ACS3+8), at $\kappa_3=141$, κ_8^H reduces to a value 920 in ACS3+8', which is less than half of the value 2178 that it reduces to in ACS3+8. Thus a larger degree of overlap between the catalyzed reaction sets of nested ACSs causes more effective reinforcement.

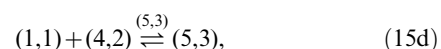
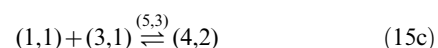
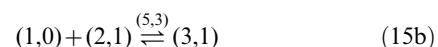
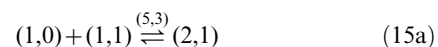
Another example with this behaviour for $f=2$ is described in Fig. 12 (for a pictorial representation of the network see Supporting Fig. S1). In each of the three ACS pairs shown in the figure, the smaller ACS, of length 4, is the same, (it will be referred to as ACS(2,2)) and is defined by the reactions (each catalyzed by (2,2))



The three larger ACSs, called ACS(5,3)(a), ACS(5,3)(b) and ACS(5,3)(c), respectively, can essentially be determined from the figure. For example, ACS(5,3)(a) consists of the two reaction pairs given by Eqs. (13), both catalyzed by (5,3) as well as the three reactions



ACS(5,3)(b) consists of the single reaction pair given by the first of Eqs. (13), catalyzed by (5,3), as well as the four reactions



and ACS(5,3)(c) consists of the five reaction pairs

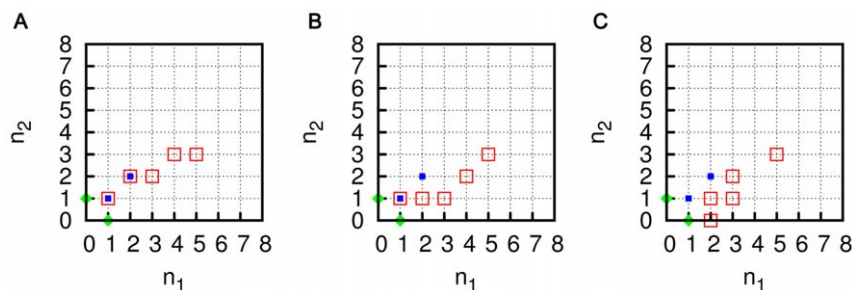
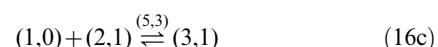
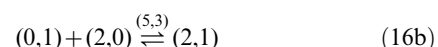
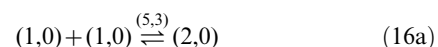
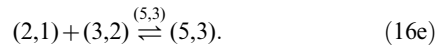
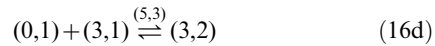


Figure 12. Examples of nested ACS pairs with different degrees of overlap for $f=2$. In the three cases the reaction sets have (A) maximal overlap, (B) partial overlap, (C) no overlap. The blue and red squares marking the grid points indicate the identity of molecules produced in the two ACSs; blue filled squares correspond to the products of the smaller ACS, red unfilled squares to those of the larger ACS. The x and y axes denote the number of monomers of type (1,0) and (0,1), respectively, in the molecules. The green rhombuses represent the two monomers. doi:10.1371/journal.pone.0029546.g012



We consider the population dynamics of chemistries in which the spontaneous part includes all possible ligation and cleavage reactions involving molecules with upto $N=15$ monomers with homogeneous rate constants $k_f=k_r=1$, $\phi=15$, and the catalyzed part containing one or more of the above mentioned ACSs. When ACS(2,2) is the only ACS present, the system shows bistability with the initiation threshold being $\kappa_{(2,2)}^H=551$. When ACS(5,3)(a), (b) or (c) are the only ACSs present, the initiation thresholds for them are 1125197, 1031082, and 1000112, respectively. When ACS(2,2) and one of ACS(5,3) (a), (b) or (c) are both present, and the catalytic strength of (2,2) is 552, the initiation thresholds of the three larger ACSs reduce to 941, 1256, and 2482, respectively. Again, it is seen that the larger the degree of overlap of the two nested ACSs, the more effective is the reinforcement.

A hierarchy of nested ACSs: A possible route for the appearance of large molecules

The process of nesting discussed above for two ACSs can be extended to multiple levels of ACSs connected to each other. Here we discuss sequences of ACSs of increasing size, with the catalyzed reaction set of each ACS in the sequence partially or completely contained within the next one, and the catalytic strength of molecules increasing with size in a controlled manner. We construct examples of such sequences in which large catalyst molecules containing several hundred monomers can acquire significant concentrations starting from the standard initial condition, even though all catalysts have moderate catalytic strengths.

In order to construct a cascade of nested ACSs in which reaction sets of smaller ACSs are completely contained in the larger ones (maximal overlap), we used Algorithm 4 described in Methods. This algorithm produces a cascade of ACSs with g steps (generations), with the k^{th} generation ACS containing n_k new reactions. We studied several catalyzed chemistries containing a

cascade of nested ACSs for $f=1$ and 2. One example of each type is presented below; other examples gave qualitatively similar results.

Dominance of an ACS of length 441 (ACS441)

For $f=1$ we describe a cascade with $g=15$ and $n_1=1, n_2=n_3=\dots=n_{15}=2$. This catalyzed chemistry had 29 product molecules, the largest of which was $A(441)$ having 441 monomers. The list of molecules and reactions is given in Table S2. The catalytic strength κ of each molecule was chosen by an explicit length dependent rule

$$\kappa(L) = KL^\beta, \quad (17)$$

where K and β are constants. We describe a simulation with $K=500$ and $\beta=1.5$. This particular rule was chosen to contrast with Eq. (9) which characterizes the initiation threshold of an extremal ACS of length L . For a value of L such as 441, the exponential function in Eq. (9) would have given an astronomically large catalytic strength, whereas the much slower growing power law in Eq. (17) gives $\kappa(441)=4.6 \times 10^6$ for the above mentioned values of the constants. Starting from the standard initial condition, the steady state concentration profile of this catalyzed chemistry embedded in a fully connected spontaneous chemistry with $N=800$ is shown in Fig. 13A. This example shows that with the nested ACS structure in the catalyzed chemistry, large catalyst molecules can acquire significant concentrations starting from an initial condition containing only the monomers, even when catalytic strengths grow quite slowly with the length of the catalyst. It is worth noting that product of the catalytic strength of $A(441)$ and its steady state concentration ($x_{441}=0.0077$) is about 36000, and this is the factor by which it speeds up the reactions it catalyzes over the spontaneous rate. In view of the fact that enzymes containing a few hundred amino acids speed up the reactions they catalyze within cells by factors of about 10^5 and greater, the catalytic efficiency demanded of $A(441)$ does not seem unreasonably high.

Eq. (17), which gives a particular functional form for $\kappa(L)$, is ad-hoc, and, at this stage, merely an example given to quantify the level of catalytic strengths that is sufficient for large molecules to arise in appreciable concentrations in the prebiotic scenario under consideration if chemistry has the nested ACS structure of the kind discussed. One may ask if an even weaker requirement would

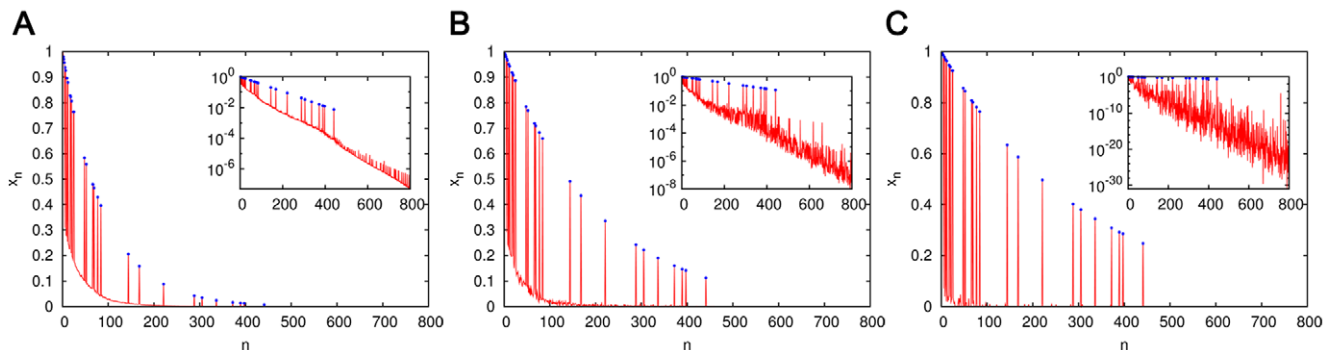


Figure 13. The dominance of a cascade of nested ACSs with a molecule of size 441 (ACS441). The molecules and reactions of this ACS are listed in Table S2. The red curves show the steady state concentration x_n of all the molecules as a function of their size n , starting from the standard initial condition; blue dots show the concentrations of the ACS molecules. The catalytic strengths of the ACS molecules depend upon their size n according to $\kappa(n)=500 \times n^{1.5}$, and for all cases $k_f=k_r=1$, $\phi=50$, $N=800$. The three figures differ in the level of sparseness of the spontaneous chemistry in which the ACS is embedded. The spontaneous chemistry in (A) is fully connected, in (B) has degree 20, and in (C) has degree 2. doi:10.1371/journal.pone.0029546.g013

suffice. We have considered smaller values of β (1.2 and 1.0) keeping K fixed, and found that ACS molecules up to a particular size (depending on β) do well but that the concentration of larger ACS molecules trails off and merges with the background. The size range of ACS molecules that do well can be increased by increasing the coefficient K . Since the results depend upon several factors, including the topology of the ACS and the uncatalyzed chemistry, a detailed investigation has not been carried out.

Effect of a 'sparse' spontaneous chemistry

Fig. 13 also shows another aspect of ACS dynamics – the relationship between ACS domination and the sparseness of the uncatalyzed chemistry. A fully connected uncatalyzed chemistry is one in which all possible ligation and cleavage reactions are allowed. A chemistry with average degree k is one in which the average number of ligation reactions in which a molecule can be produced is k . In a fully connected $f=1$ chemistry, a molecule of size n can be produced in about $n/2$ ligation reactions ($A(1)+A(n-1)\rightarrow A(n)$, $A(2)+A(n-2)\rightarrow A(n)$, etc.); therefore the average degree of a chemistry containing all molecules up to size N is about $N/4$ ($=200$ for the chemistry in Fig. 13A). In Figs. 13B and 13C, we pruned the uncatalyzed reaction set to only k ligation reactions per molecule ($k=20$ and 2 , respectively), randomly chosen from all possible ligation reactions producing the molecule. (For molecules too small to have k ligation reactions, all ligation reactions were retained. For the ACS molecules the ligation reaction producing them in the catalyzed chemistry was included as one of the k uncatalyzed reactions.) Note that while we refer to only the ligation reactions and not cleavage reactions for the purpose of defining the degree of a molecule, in our simulations all reactions are treated as reverse reactions. That is, for every ligation reaction included in the chemistry the reverse (cleavage) reaction is also present. It is seen in Fig. 13 that the increase of sparseness causes the background concentrations to decline. This is because there are fewer pathways to produce the background molecules. There is also a larger variation in their concentrations because their production reactions are chosen randomly, and background molecules produced in reactions that happen to involve the ACS molecules as reactants do better than others. The ACS molecules are seen to dominate more strongly over the background in sparser chemistries; this is because there

are fewer production pathways to the background that drain their concentrations.

Cascading nested ACSs with $f=2$

An example of a nested ACS with two food sources, ACS(36,28), is presented in Fig. 14. This is also generated by Algorithm 4 and has 7 generations with $n_k=3$ for each generation, the largest molecule being (36,28) (the full list of molecules and reactions is given in Table S3). Again starting from the standard initial condition the larger ACS molecules acquire appreciable concentrations with a moderate demand on their catalytic strengths.

As a final example we present in Fig. 15 a cascade of ACSs, named ACS(18,27) after its largest molecule, in which smaller ACSs have only a partial overlap with longer ones. This is generated using Algorithm 5 (see Methods) and consists of a series of 10 ACSs of increasing length. The detailed list of molecules, reactions and catalytic strengths is given in Table S4. Each successive ACS in the cascade has only a few reactions in common with other ACSs. Unlike in the examples discussed above, generated by Algorithm 4, in the present case molecules (except the small molecules) produced in the catalyzed chemistry have typically only one or two catalyzed ligation reactions producing them. The chemistry also contains a number of catalyzed 'side reactions', which produce molecules that are neither catalysts nor reactants in any pathway leading to the largest molecule. In fact there is a 'side pathway' consisting of several reactions that may be viewed as 'draining the resources' of the main ACS. ACS dominance at moderate catalytic strengths occurs for this chemistry also. The largest κ is 50000 for the molecule (18,27), and at a steady state population of 0.26 enhances the rate of a reaction by a factor of 13000 over the spontaneous rate. This shows that the mechanism outlined by us is not restricted to maximally overlapping nested ACSs but is more generic.

Discussion

Our work discusses a possible mechanism by which large molecules can arise in a prebiotic scenario. In the context of the present model the appearance of large molecules is a natural dynamical consequence of chemistry possessing the structure

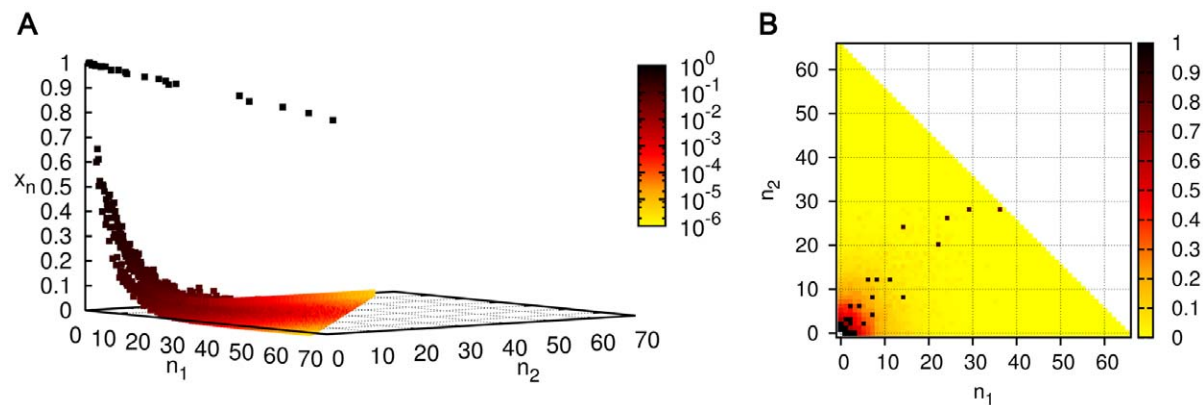


Figure 14. Dominance of a cascade of nested ACSs with length 64 (ACS(36,28)) in a $f=2$ chemistry. (A) 3D plot showing the steady state concentration x_n of the molecule $n=(n_1, n_2)$ as a function of n_1 and n_2 , starting from the standard initial condition. The colour coding is on a logarithmic scale of the concentration. (B) A 'top view' of the same so that the ACS molecules and background are more clearly distinguished. The colour coding here is on a linear scale of concentration. The food set and ACS molecules have the highest concentrations and stand out as black dots. The catalytic strengths of the ACS molecules depend upon their size $L \equiv n_1 + n_2$ according to $\kappa(L) = 500 \times L^{1.5}$, and $k_f = k_r = 1$, $\phi = 10$, $N = 65$. The spontaneous chemistry has degree 20. doi:10.1371/journal.pone.0029546.g014

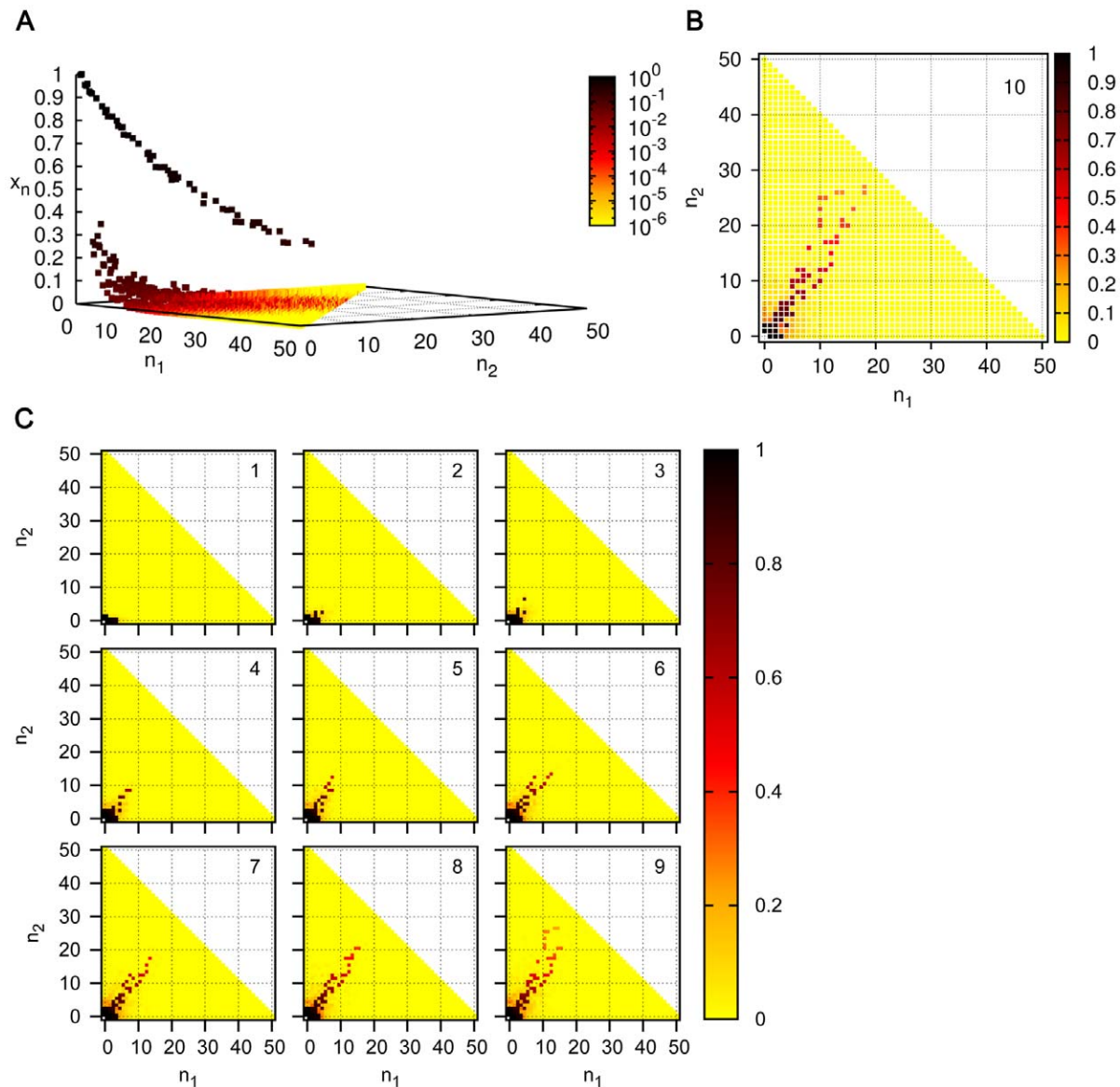


Figure 15. Dominance of a cascade of partially overlapping nested ACSs (ACS(18,27)). (A) Steady state concentration profile starting from the standard initial condition. (B) Top view of the same. (C) Sequence of steady state concentration profiles as each successive ACS is added to the chemistry. The legend for (A) is the same as for Fig. 14A and for (B) and (C) the same as Fig. 14B. $k_f = k_r = 1$, $\phi = 15$, $N = 50$, and the spontaneous chemistry has degree 5.

doi:10.1371/journal.pone.0029546.g015

described above – a cascading nested ACS structure (with a not very demanding set of catalytic strengths) embedded in a spontaneous chemistry – together with the buffered presence of the food set molecules in a well stirred region of space. The mechanism is an incremental one: at each step successive step the system is able to access new states made available by the previous step while making only an incremental demand on molecular catalytic capabilities.

The kind of mathematical model we have studied, inspired by the work of Bagley and Farmer, is quite abstract; its virtue is the economy of assumptions that go into its structure. The main ingredients are that objects can combine with each other in processes or ‘reactions’ to form other objects and certain objects can facilitate certain processes, i.e., ‘catalyze’ certain reactions. The population dynamics implements a simple scheme for how

the abundances of the objects would change with time assuming that the probability of objects combining is proportional to their abundances. Such a generic scheme while it applies in detail to no particular situation allows us to imagine mechanisms at a conceptual level. It is significant that in this scheme an ACS can direct the flows towards itself and cause a certain sparse subset of objects, including some specific large composite ones, to capture a large fraction of the chemical resources.

At this level of abstraction the model (or a variant with qualitatively similar features) could apply to the peptide chemistry as well as an RNA chemistry and to a prebiotic metabolism, as already noted by Bagley and Farmer. Indeed it would be equally applicable if a prebiotic environment actually had a mixture of ingredients from all these classes of chemistries, a possibility that has been advocated in, e.g., [51,52]. Copley, Smith and Morowitz

[51] have proposed a scenario which seeks to explain how the RNA world might have originated through a series of incremental steps starting from a primitive metabolism. The food sources for this supposed metabolism are CO_2 , H_2 , H_2S , NH_3 , etc., in a hydrothermal vent. Their scenario envisages multiple stages of increasing complexity which they refer to as (i) the monomer stage, in which metabolism, possibly powered by an autocatalytic set such as the reverse TCA cycle, produces nucleotides and simple amino acids, (ii) the multimer stage, which produces dimers and small cofactors, (iii) the micro-RNA stage, producing of oligonucleotides of length 3–10, (iv) the mini-RNA stage, with 11–40 mers, followed by (v) the macro-RNA stage, or the RNA world. In their scenario each successive stage produced better catalysts that collectively catalyzed not only their own production from the molecules of the previous stage, but also the reactions of the lower stages. This structure is very similar to the cascade of nested ACSs that we have discussed. A suitably modified version of our model could be constructed to explore the dynamics of this scenario in more detail. At a general level, in the fact that the dynamics of our model results in the stable domination, or concentrating, of the large catalysts, our mathematical work perhaps lends support to the workability of such a scenario.

There is another level at which the present model (or its variants) might talk to prebiotic chemistry. Morowitz [53] has suggested that the metabolic network itself has a shell like structure which can convert simple molecules like CO_2 , H_2 , NH_3 , etc., through “a hierarchy of nested reaction networks involving increasing complexity” into purines, pyrimidines, complex cofactors, etc. Reaction sets created by our Algorithms 4 and 5 are reminiscent of this picture. Missing from Morowitz’s picture is a catalyst assignment for each reaction from among the molecules in the various shells or from among other catalysts accessible prebiotically (e.g., surfaces in hydrothermal vents). It might be worthwhile to attempt to add in that information for a more complete scenario and for potential modeling.

Caveats and future directions

(1) We have studied the properties of autocatalytic systems, by choosing specific examples of ACS topology and special algorithms for constructing them. This has allowed us to systematically investigate the dynamical properties that ACSs offer. We believe that similar dynamical properties would hold for more general topological structures than we have considered. Nevertheless the question arises as to whether all these structures are very special structures and whether or not they are likely to arise within real chemistry and ‘generic’ artificial chemistries. ACSs have been shown to be quite generic in a large class of randomly constructed artificial chemistries [54,55], and a similar analysis could be extended to cascading nested ACSs. This would help parametrize or characterize chemistries that would contain such structures and those that would not. In this context it would be useful to go beyond the simple case we have considered in which a molecule is defined by the number of monomers of each type and not their sequence. It may also be interesting to look for structures similar to nested ACSs in real metabolic networks using methods similar to those in [56].

(2) An important related question is one of side reactions (discussed in [57,58]) which might destroy the efficacy of ACSs. In the real chemistry one expects that even if cascading nested ACSs exist, there would also exist other catalyzed reactions channelizing the ACS products into pathways leading in other directions. Whether substantial populations of large molecules in the nested ACSs can be maintained in the presence of such diversion is a question that remains to be systematically investigated. Our last

example of cascading nested ACSs in fact has several side reactions and it may be noted that large ACSs still dominated in that case. We remark that while side reactions can drain resources from ACSs, they also help the system to explore new directions in chemical space in an evolutionary scenario.

(3) We have considered deterministic dynamics in this paper. Stochastic fluctuations are important when molecular populations are small. For a chemistry containing multiple ACSs, Bagley, Farmer and Fontana [24] used stochasticity to produce examples of trajectories that differed from each other in the sequence of ACSs that came to dominate the reactor. It would be interesting to explore such effects in the context of the present model.

(4) Another simplification we have made is that of homogeneous chemistries, wherein the rate constants of all spontaneous reactions have been taken to be the same, and even catalytic strengths, where variable, have been taken to be smooth functions of the length. We have checked that introducing a small amount of heterogeneity or randomness in the rate constants does not change the qualitative behaviour significantly. However, the effect of cranking up the heterogeneity has not been studied. From studies of disordered systems in statistical mechanics and condensed matter physics it has become clear that such heterogeneity can lead to rugged landscapes, multiple attractors and timescales, and paths that are difficult to locate [59]. The dynamics of such systems when they are driven by a non-equilibrium flux or buffering of food set molecules is an open question. It is possible that the constraints placed by the ruggedness of the landscape will reduce the number of accessible paths. The populating of molecules at different levels in a nested hierarchy of ACSs is likely to happen in fits and starts on multiple timescales when heterogeneity is accounted for. It is perhaps in such a scenario that one should look for answers to the questions raised under (1), (2) and (3) above.

Methods

A. Generating extremal ACSs of length L

In the following we describe three different algorithms used for generating a set of reactions that provide a pathway to produce a molecule of a given length L from the food set.

Algorithm 1: Incremental, smallest-stepsize, deterministic construction. Each molecule of size n ($n=2,3,\dots,L$) is produced in the reaction $A(1)+A(n-1)\rightarrow A(n)$. All such reactions for $n=2,3,\dots,L$ are included in the ACS.

Algorithm 2: Shortest path, top-down, deterministic construction. Start with $A(L)$. If L is even, it is produced in the reaction $A(L/2)+A(L/2)\rightarrow A(L)$. If L is odd, say $L=2m+1$, then $A(L)$ is produced in the reaction $A(m)+A(m+1)\rightarrow A(L)$. The same algorithm is used to select a reaction for the production of the precursor(s) of $A(L)$ (namely, for $A(L/2)$ if L is even, and for each of $A(m)$ and $A(m+1)$ if L is odd ($=2m+1$)), and is iterated for their precursors, etc., until the only reactant appearing in the reactions is the food set molecule, $A(1)$. All the production reactions mentioned above are included in the ACS.

Algorithm 3: Incremental, random construction. In this method, starting from the food set \mathcal{F} the set of reactants R_k is sequentially enlarged step by step ($\mathcal{F}=R_0\subset R_1\subset R_2\subset\dots$) to include larger molecules and a reaction chosen randomly until a product of length L is obtained. R_k denotes the set of reactants at step k in the algorithm, and L_k the size of the largest molecule in R_k . At step k , pick a pair of molecules (say X and Y) randomly from R_k , and determine the product Z formed if they were to be ligated (X being the same as Y is allowed). If the size of this product, $L(Z)$, is $\leq L_k$ or $>L$, discard the pair and choose

another pair. If $L_k < L(Z) < L$, add the ligation reaction $X + Y \rightarrow Z$ to the ACS, define $R_{k+1} = R_k \cup \{Z\}$, and iterate the procedure. If $L(Z) = L$, add the ligation reaction $X + Y \rightarrow Z$ to the ACS, and stop. Initially ($k=0$) the reactant set is just the food set, $R_0 = \mathcal{F}$.

To complete the extremal ACS, we assign $A(L)$ as the catalyst of all the reactions generated using any of the above algorithms. For the simulations reported in the paper, the reverse of each reaction is also included as a reaction catalyzed by the same catalyst. For concreteness we have described the Algorithms 1 and 2 for the single monomer case; their generalizations to $f=2$ have also been considered by us. Algorithm 3, as described above, can be used for any f .

B. Generating a cascade of nested ACSs

Algorithm 4: Incremental, random construction of a sequence of reaction sets with maximal overlap. We construct successive sets, or ‘generations’, g in number, P_1, P_2, \dots, P_g , of product molecules, starting from the food set $\mathcal{F} (\equiv P_0)$. Each generation P_k ($k=1, 2, \dots, g$) has a pre-specified number of molecules, n_k (n_1, n_2, \dots, n_g need to be specified before running the algorithm). At step k of the cascade an ACS S_k is constructed from the previous ACS S_{k-1} by adding reactions between molecules belonging to a reactant set R_k consisting of all the products of the previous generations and the food set, $R_k = P_0 \cup P_1 \cup P_2 \dots P_{k-1}$. Let L_k denote the size of the largest molecule in R_k . At the beginning of the k^{th} step, P_k is empty and the set of reactions in S_k is the same as in S_{k-1} , except that the catalysts of the reactions in S_k are not yet assigned. (S_0 is the empty set.) To construct P_k and S_k , pick a molecule X at random from the previous generation of products P_{k-1} and another molecule Y at random from R_k , and determine the product Z formed if they were to be ligated (X being the same as Y is allowed). If the size of this product, $L(Z)$, is $\leq L_k$, discard the pair and choose another pair. If $L(Z) > L_k$, add the molecule Z to P_k and the ligation reaction $X + Y \rightarrow Z$ to S_k . Repeat this procedure until n_k molecules are added to P_k and n_k reactions are added to S_k . Assign catalysts to each reaction in S_k (which includes the reactions inherited from S_{k-1} and the new n_k reactions) randomly from P_k . This completes the k^{th} step. To get the full cascade with g generations this process is carried out for $k=1, 2, \dots, g$. By construction the set of reactions (ignoring the catalyst) of each S_k is fully contained in that of S_{k+1} but the catalysts are different, being drawn from P_k for S_k and P_{k+1} for S_{k+1} . The union of the S_k 's constitutes the set of reactions in the catalyzed chemistry. Note that in this catalyzed chemistry reactions have multiple catalysts, the multiplicity declining for reactions producing higher generation molecules.

The size of the food set constrains how large n_k can be. For $f=1$, $n_1=1$ and $P_1 = \{A(2)\}$ as the only product one can make from a reaction in the food set is $A(1) + A(1) \rightarrow A(2)$, and n_2 can only have values 1 and 2 as the only products one can produce in the second generation (from reactants in $R_2 = \{A(1), A(2)\}$) are $A(3)$ and $A(4)$, etc. Similarly for $f=2$, n_1 can be only 1, 2 or 3, as reactions among the two food set molecules (1,0) and (0,1) can only produce three molecules (2,0), (1,1) and (0,2).

Algorithm 5: Incremental, random construction of a sequence of reaction sets with partial overlap. In this

algorithm we decide on a sequence of lengths, L_1, L_2, \dots, L_g , and generate an extremal ACS, denoted S_i , of length L_i using Algorithm 3 for each $i=1, 2, \dots, g$. For each i a different random number seed is used to initialize Algorithm 3. The union of the S_i 's constitutes the set of reactions in the catalyzed chemistry.

C. Computer programs

The chemistries, spontaneous and catalyzed (including the ACSs mentioned above), are generated in C programs which are available from the authors upon request. These programs further use the CVODE library to do the numerical integration of the differential equations and also generate the inputs files required for XPPAUT, Octave and Mathematica.

Supporting Information

Figure S1 Pictorial representation of nested ACSs with $f=2$. Each of the three figures shows two nested ACSs. The smaller ACS in each figure is ACS(2,2), defined by Eqs. (0) in the main text. The larger ACS is different and is given by (A) ACS(5,3)(a), (B) ACS(5,3)(b), and, (C) ACS(5,3)(c), defined in the main text below Eqs. (13). The notation is the same as in Figs. 3 and 9 of the main text.

(TIF)

Table S1 List of reactions and their catalysts in ACS(8,10) referred in Fig. 5.

(PDF)

Table S2 List of reactions and their catalysts in ACS441 referred in Fig. 13.

(PDF)

Table S3 List of reactions and their catalysts in ACS(36,28) referred in Fig. 14.

(PDF)

Table S4 List of reactions and their catalysts in ACS(18,27) referred Fig. 15.

(PDF)

Appendix S1 Details of the general model and explicit examples for $f=1$ and 2.

(PDF)

Appendix S2 N -independence of results at large N .

(PDF)

Appendix S3 Dimensionless rate equations and dependence of Λ on dimensionless parameters.

(PDF)

Acknowledgments

We would like to thank Eric Smith for drawing our attention to the paper of Ohtsuki and Nowak (ref. [34]) and Shobhit Mahajan, Amitabha Mukherjee and Awadhesh Prasad for discussions.

Author Contributions

Analyzed the data: SJ VG. Wrote the paper: SJ VG. Conceived the research: SJ. Designed the research: VG SJ. Performed simulations: VG.

References

1. Miller SL (1953) A production of amino acids under possible primitive earth conditions. *Science* 117: 528–529.
2. Miller SL, Urey HC (1959) Organic compound synthesis on the primitive earth. *Science* 130: 245–251.
3. Ricardo A, Carrigan MA, Olcott AN, Benner SA (2004) Borate minerals stabilize ribose. *Science* 303: 196.
4. Powner MW, Gerland B, Sutherland JD (2009) Synthesis of activated pyrimidine ribonucleotides in prebiotically plausible conditions. *Nature* 459: 239–242.

5. Parker ET, Cleaves HJ, Dworkin JP, Glavin DP, Callahan M, et al. (2011) Primordial synthesis of amines and amino acids in a 1958 Miller H₂S-rich spark discharge experiment. *Proceedings of the National Academy of Sciences (USA)* 108: 5526–5531.
6. Rode BM (1999) Peptides and the origin of life. *Peptides* 20: 773–786.
7. Ferris JP, Joshi PC, Wang K, Miyakawa S, Huang W (2004) Catalysis in prebiotic chemistry: Application to the synthesis of RNA oligomers. *Advances in Space Research* 33: 100–105.
8. Orgel LE (2004) Prebiotic chemistry and the origin of the RNA world. *Critical Reviews in Biochemistry and Molecular Biology* 39: 99–123.
9. Budin I, Szostak JW (2010) Expanding roles for diverse physical phenomena during the origin of life. *Annual Review of Biophysics* 39: 245–263.
10. Barbas CF (2008) Organocatalysis lost: Modern chemistry, ancient chemistry, and an unseen biosynthetic apparatus. *Angewandte Chemie International Edition* 47: 42–47.
11. MacMillan DWC (2008) The advent and development of organocatalysis. *Nature* 455: 304–308.
12. Bertelsen S, Jorgensen KA (2009) Organocatalysis—after the gold rush. *Chemical Society Reviews* 38: 2178–2189.
13. Severin K, Lee DH, Kennan AJ, Ghadiri MR (1997) A synthetic peptide ligase. *Nature* 389: 706–709.
14. Brack A (2007) From interstellar amino acids to prebiotic catalytic peptides: A review. *Chemistry & Biodiversity* 4: 665–679.
15. Cech TR, Bass BL (1986) Biological catalysis by RNA. *Annual Review of Biochemistry* 55: 599–629.
16. Symons RH (1992) Small catalytic RNAs. *Annual Review of Biochemistry* 61: 641–671.
17. Chen X, Li N, Ellington AD (2007) Ribozyme catalysis of metabolism in the RNA world. *Chemistry & Biodiversity* 4: 633–655.
18. Srinivasan V, Morowitz HJ (2009) Analysis of the intermediary metabolism of a reductive chemoautotroph. *The Biological Bulletin* 217: 222–232.
19. Eigen M (1971) Selforganization of matter and the evolution of biological macromolecules. *Die Naturwissenschaften* 58: 465–523.
20. Kauffman SA (1971) Cellular homeostasis, epigenesis and replication in randomly aggregated macromolecular systems. *Journal of Cybernetics* 1: 71–96.
21. Rössler OE (1971) A system theoretic model for biogenesis. *Zeitschrift für Naturforschung. Teil B: Chemie, Biochemie, Biophysik, Biologie* 26: 741–746.
22. Farmer JD, Kauffman SA, Packard NH (1986) Autocatalytic replication of polymers. *Physica D: Nonlinear Phenomena* 22: 50–67.
23. Bagley RJ, Farmer JD (1991) Spontaneous emergence of a metabolism. In: Langton CG, Taylor CE, Farmer JD, Rasmussen S, eds. *Artificial Life II*, Addison-Wesley. pp 93–140.
24. Bagley RJ, Farmer JD, Fontana W (1991) Evolution of a metabolism. In: Langton CG, Taylor CE, Farmer JD, Rasmussen S, eds. *Artificial Life II*, Addison-Wesley. pp 141–158.
25. Stadler P, Fontana W, Miller J (1993) Random catalytic reaction networks. *Physica D: Nonlinear Phenomena* 63: 378–392.
26. Kauffman SA (1993) *The origins of order: Self-organization and selection in evolution*. New York: Oxford University Press.
27. Fontana W, Buss LW (1994) What would be conserved if “the tape were played twice”? *Proceedings of the National Academy of Sciences (USA)* 91: 757–761.
28. Jain S, Krishna S (1998) Autocatalytic sets and the growth of complexity in an evolutionary model. *Physical Review Letters* 81: 5684–5687.
29. Jain S, Krishna S (2001) A model for the emergence of cooperation, interdependence, and structure in evolving networks. *Proceedings of the National Academy of Sciences (USA)* 98: 543–547.
30. Hanel R, Kauffman S, Thurner S (2005) Phase transition in random catalytic networks. *Physical Review E* 72: 036117.
31. Piedrafita G, Montero F, Morán F, Cárdenas ML, Cornish-Bowden A (2010) A simple selfmaintaining metabolic system: Robustness, autocatalysis, bistability. *PLoS Computational Biology* 6: e1000872.
32. Eigen M, Schuster P (1977) The hypercycle: A principle of natural self-organization. Part A: Emergence of the hypercycle. *Die Naturwissenschaften* 64: 541–565.
33. Szathmáry E (2006) The origin of replicators and reproducers. *Philosophical Transactions of the Royal Society B* 361: 1761–1776.
34. Ohtsuki H, Nowak MA (2009) Pre-life catalysts and replicators. *Proceedings of the Royal Society B* 276: 3783–3790.
35. Segré D, Ben-Eli D, Lancet D (2000) Compositional genomes: prebiotic information transfer in mutually catalytic noncovalent assemblies. *Proceedings of the National Academy of Sciences (USA)* 97: 4112–4117.
36. Furusawa C, Kaneko K (2006) Evolutionary origin of power-laws in a biochemical reaction network: Embedding the distribution of abundance into topology. *Physical Review E* 73: 011912.
37. Carletti T, Serra R, Poli I, Villani M, Filisetti A (2008) Sufficient conditions for emergent synchronization in protocell models. *Journal of Theoretical Biology* 254: 741–751.
38. Kamimura A, Kaneko K (2010) Reproduction of a protocell by replication of a minority molecule in a catalytic reaction network. *Physical Review Letters* 105: 268103.
39. Bagley RJ, Farmer JD, Kauffman SA, Packard NH, Perelson AS, et al. (1989) Modeling adaptive biological systems. *Bio Systems* 23: 113–137.
40. Wächtershäuser G (1990) Evolution of the first metabolic cycles. *Proceedings of the National Academy of Sciences (USA)* 87: 200–204.
41. Morowitz HJ, Kostelnik JD, Yang J, Cody GD (2000) The origin of intermediary metabolism. *Proceedings of the National Academy of Sciences (USA)* 97: 7704–7708.
42. Hindmarsh AC, Brown PN, Grant KE, Lee SL, Serban R, et al. (2005) SUNDIALS: Suite of nonlinear and differential/algebraic equation solvers. *ACM Transactions on Mathematical Software* 31: 363–396.
43. Ermentrout B (2002) *Simulating, Analyzing, and Animating Dynamical Systems: A Guide to XPPAUT for Researchers and Students*. Philadelphia: Society for Industrial Mathematics, first edition, 290. Available: <http://www.math.pitt.edu/~bard/xpp/xpp.html>.
44. Octave. Available: <http://www.gnu.org/software/octave>.
45. Wolfram Research, Inc. (2008) *Mathematica*, Version 7.0. Champaign, Illinois.
46. Craciun G, Tang Y, Feinberg M (2006) Understanding bistability in complex enzyme-driven reaction networks. *Proceedings of the National Academy of Sciences (USA)* 103: 8697–8702.
47. Angeli D, Hirsch MW, Sontag ED (2009) Attractors in coherent systems of differential equations. *Journal of Differential Equations* 246: 3058–3076.
48. Craciun G, Pantea C, Sontag ED (2011) Graph-Theoretic Analysis of Multistability and Monotonicity for Biochemical Reaction Networks. In: Koeppl H, Setti G, di Bernardo M, Densmore D, eds. *Design and Analysis of Biomolecular Circuits: Engineering Approaches to Systems and Synthetic Biology*. New YorkNY: Springer. pp 63–72.
49. Wilhelm T (2007) Analysis of structures causing instabilities. *Physical Review E* 76: 011911.
50. Ramakrishnan N, Bhalla US (2008) Memory switches in chemical reaction space. *PLoS computational biology* 4: e1000122.
51. Copley SD, Smith E, Morowitz HJ (2007) The origin of the RNA world: co-evolution of genes and metabolism. *Bioorganic Chemistry* 35: 430–443.
52. Powner MW, Sutherland JD (2011) Prebiotic chemistry: A new modus operandi. *Philosophical Transactions of the Royal Society B* 366: 2870–2877.
53. Morowitz HJ (1999) A theory of biochemical organization, metabolic pathways, and evolution. *Complexity* 4: 39–53.
54. Steel M (2000) The emergence of a self-catalysing structure in abstract origin-of-life models. *Applied Mathematics Letters* 13: 91–95.
55. Hordijk W, Kauffman SA, Steel M (2011) Required levels of catalysis for emergence of autocatalytic sets in models of chemical reaction systems. *International journal of molecular sciences* 12: 3085–3101.
56. Kun A, Papp B, Szathmáry E (2008) Computational identification of obligatorily autocatalytic replicators embedded in metabolic networks. *Genome biology* 9: R51.
57. Orgel LE (2000) Self-organizing biochemical cycles. *Proceedings of the National Academy of Sciences (USA)* 97: 12503–12507.
58. Orgel LE (2008) The implausibility of metabolic cycles on the prebiotic earth. *PLoS biology* 6: e18.
59. Wales DJ (2004) *Energy landscapes: Applications to clusters, biomolecules and glasses* Cambridge University Press. 692 p. doi:10.2277/0521814154.